CD248 promotes insulin resistance by binding to the insulin receptor and dampening its insulin-induced autophosphorylation

Patricia O. Benedet,[a,b] Nooshin S. Safikhan,[a,b] Maria J. Pereira,[d] Bryan M. Lum,[c] José Diego Botezelli,[a,b] Cheng-Hsiang Kuo,[g] Hua-Lin Wu,[h] Barbara P. Craddock,[e] W. Todd Miller,[e,f] Jan W. Eriksson,[d] Jessica T. Y. Yue,[c] and Edward M. Conway[a,b,*]

[a]Centre for Blood Research, Life Sciences Institute, Faculty of Medicine, University of British Columbia, Vancouver, Canada
[b]Departments of Medicine and Pathology and Laboratory Medicine, Life Sciences Institute, Faculty of Medicine, University of British Columbia, Vancouver, Canada
[c]Department of Physiology, Alberta Diabetes Institute and Group on Molecular and Cell Biology of Lipids, University of Alberta, Canada
[d]Department of Medical Sciences, Clinical Diabetology & Metabolism, Uppsala University, Sweden
[e]Department of Physiology and Biophysics, Stony Brook University, Stony Brook, NY, USA
[f]Veterans Affairs Medical Center, Northport, NY, USA
[g]International Center for Wound Repair and Regeneration, National Cheng Kung University, Tainan, Taiwan
[h]Department of Biochemistry and Molecular Biology, College of Medicine, National Cheng Kung University, Tainan, Taiwan

Summary

Background In spite of new treatments, the incidence of type 2 diabetes (T2D) and its morbidities continue to rise. The key feature of T2D is resistance of adipose tissue and other organs to insulin. Approaches to overcome insulin resistance are limited due to a poor understanding of the mechanisms and inaccessibility of drugs to relevant intracellular targets. We previously showed in mice and humans that CD248, a pre/adipocyte cell surface glycoprotein, acts as an adipose tissue sensor that mediates the transition from healthy to unhealthy adipose, thus promoting insulin resistance.

Methods Molecular mechanisms by which CD248 regulates insulin signaling were explored using *in vivo* insulin clamp studies and biochemical analyses of cells/tissues from CD248 knockout (KO) and wild-type (WT) mice with diet-induced insulin resistance. Findings were validated with human adipose tissue specimens.

Findings Genetic deletion of CD248 in mice, overcame diet-induced insulin resistance with improvements in glucose uptake and lipolysis in white adipose tissue depots, effects paralleled by increased adipose/adipocyte GLUT4, phosphorylated AKT and GSK3β, and reduced ATGL. The insulin resistance of the WT mice could be attributed to direct interaction of the extracellular domains of CD248 and the insulin receptor (IR), with CD248 acting to block insulin binding to the IR. This resulted in dampened insulin-mediated autophosphorylation of the IR, with reduced downstream signaling/activation of intracellular events necessary for glucose and lipid homeostasis.

Interpretation Our discovery of a cell-surface CD248-IR complex that is accessible to pharmacologic intervention, opens research avenues toward development of new agents to prevent/reverse insulin resistance.

Funding Funded by Canadian Institutes of Health Research (CIHR), Natural Sciences and Engineering Research Council of Canada (NSERC), Canada Foundations for Innovation (CFI), the Swedish Diabetes Foundation, Family Ernfors Foundation and Novo Nordisk Foundation.

Keywords: Adipocyte; Insulin resistance; Glucose; Metabolism; Obesity; CD248; Lipid; Insulin receptor

*Corresponding author. Centre for Blood Research, Life Sciences Institute, 4306-2350, Health Sciences Mall, University of British Columbia, Vancouver, British Columbia, V6T 1Z3, Canada.
E-mail address: ed.conway@ubc.ca (E.M. Conway).

Research in context

Evidence before this study

Type 2 diabetes (T2D) is an increasingly common, chronic inflammatory disorder that is strongly linked to a heightened risk of multiple disorders, including coronary heart disease, peripheral vascular disease, stroke, retinopathy, kidney failure and cancer. The central mechanism underlying T2D is resistance of key organs, including adipose tissue, to the activities of insulin. Insulin normally mediates its effects on glucose and lipid metabolism by binding to a cell surface-expressed insulin receptor and inducing its autophosphorylation, whereupon a cascade of intracellular events are triggered that maintain metabolic homeostasis. Current understanding of the mechanisms of insulin resistance is limited, but has been focused on disturbances in the function(s) of intracellular components of the insulin cascade. Drugs that can access these targets are challenging to develop, and thus there are currently none in clinical use for T2D that specifically overcome insulin resistance. Identification of pathways that regulate insulin sensitivity that are more accessible to pharmacologic intervention would predictably be of huge value.

CD248 is a transmembrane glycoprotein that is expressed on the surface of pre/adipocytes. We recently showed that CD248 is a sensitive marker of adipocyte function, increased levels of which in humans and mice, result in disturbances in glucose and lipid metabolism, and which are tightly correlated with insulin resistance and obesity. Deletion of CD248 in murine adipocytes reduces white adipose tissue hypoxia, inflammation and fibrosis, and improves glucose tolerance and insulin sensitivity. The mechanisms by which this cell-surface expressed glycoprotein, CD248, modulates insulin sensitivity, has not been explored.

Added value of this study

Our findings add considerably to our current body of knowledge of the impact of CD248 on insulin signaling and glucose and lipid metabolism, and uncover an entirely new and more readily accessible strategy to treat T2D.

Using the gold-standard insulin clamps in diet-induced insulin resistant mice, we first determined that lack of CD248 improves glucose metabolism by enhancing insulin sensitivity in the liver to suppress glucose production and in white adipose tissue to stimulate glucose uptake. The effects on glucose uptake were validated *ex vivo* in tissue explant experiments, where we also showed that CD248 interferes with insulin-induced lipolysis in white adipose tissue. Explaining these CD248-dependent effects on metabolism, Western blot analyses of adipose tissue and primary pre/adipocytes from the mice demonstrated that CD248 interferes with the two canonical insulin signaling pathways, i.e., via the Ras/MAPK pathway and the AKT-PI3 kinase (PI3K) pathway. These effects were evident in males and to a lesser extent in females, as well as in primary adipocytes from obese humans. Involvement of both canonical pathways suggested that CD248 acts "high up" in modulating insulin signaling. Our investigations then led to the major discoveries that the extracellular domains of CD248 interact directly with the extracellular region of the insulin receptor, and that CD248 blocks insulin binding to the insulin receptor and dampens insulin-induced phosphorylation of the insulin receptor.

Implications of all the available evidence

This study uncovers a mechanism by which CD248 promotes insulin resistance, i.e., its presence confers resistance to insulin-induced downstream activation/phosphorylation of insulin-dependent pathways, manifest most frequently in the setting of obesity, by disorders of glucose uptake and lipid metabolism that are observed in T2D. The implications are that reversal of this insulin resistant state may be achieved by reducing CD248 expression and/or by blocking the interaction of CD248 with the insulin receptor. The fact that the interaction of CD248 and the insulin receptor occurs on the cell surface, provides a uniquely accessible potential therapeutic target to prevent/reverse insulin resistance and to improve metabolic health.

Introduction

Type 2 diabetes (T2D) is a chronic inflammatory disease that is associated with multiple morbidities, including in particular, a heightened risk of cardio-cerebro-vascular disorders, thrombosis and cancer.[1–3] More than 450 million people are living with diabetes, a number expected to grow to ~650 million by 2040. A key feature of T2D is resistance of adipose tissue and other organs to insulin, often accompanied by hyperinsulinemia.[4]

Insulin controls key metabolic activities, including inducing glucose uptake, glycogenesis and lipogenesis, inhibiting lipolysis, stimulating protein synthesis, and enhancing adipogenesis.[5–7] Its effects are mediated via cell surface-expressed tyrosine kinase receptors, triggering signaling cascades leading to a plethora of cellular responses, dysregulation of which are believed to result in the associated morbidities. Thus, for example, the increased risk of cancer in T2D is likely due in part to sustained insulin-induced signaling that promotes pathologic angiogenesis, dysregulated cell differentiation and proliferation, with alterations in cell metabolism.[8] Mechanisms that regulate insulin signaling are incompletely understood, as are those that underly insulin resistance.[9] It is known however, that with obesity and white adipose tissue (WAT) expansion, extracellular matrix remodeling occurs.[10] This is associated with inadequate angiogenesis[11] due to microenvironmental hypoxia, the latter which is accompanied by dampened adipogenesis and dysregulated expression and/or activation of the insulin receptor (IR).[12,13]

Adipocytes become dysfunctional with multiple changes, including mitochondrial disturbances, reduced adiponectin release, upregulation of pro-apoptotic and pro-fibrotic genes, increased release of cytokines and adipokines, infiltration with pro-inflammatory cells and suppression of preadipocyte differentiation.[14] The associated disturbances in glucose metabolism and insulin sensitivity may occur early, even before evidence of inflammation.

CD248 is a multi-domain, transmembrane glycoprotein expressed on the surface of pre/adipocytes, perivascular cells and macrophages. From studies with gene targeted mice, we and others showed that CD248 participates in hypoxic regulation and angiogenesis,[15–18] and promotes inflammation, fibrosis, and tumorigenesis. Mice lacking *CD248* (KO) are healthy and protected against tumor growth,[16,19,20] atherosclerosis,[21] arthritis,[16] thrombosis,[22] liver and renal fibrosis[23–25] and lipid accumulation.[26] We also recently reported that mice lacking *CD248* either globally or specifically in mature adipocytes, are resistant to high fat diet (HFD)-induced weight gain, and are protected against insulin resistance, glucose intolerance and steatosis.[18] Notably, WAT health, insulin sensitivity and glucose tolerance could be restored to normal after onset of HFD-induced diabetes by genetically excising *CD248* from the mature adipocyte. The relevance of CD248 in glucometabolic health in humans was confirmed by studies of several independent clinical cohorts, showing that CD248 expression in adipocytes strongly and directly correlates with dysfunctional WAT and insulin resistance.[18]

Our findings that CD248, a pre/adipocyte cell surface expressed protein, acts as an adipose tissue sensor that mediates the transition from healthy to unhealthy adipose, thus promoting an insulin resistant state, prompted us to investigate the underlying molecular mechanisms. In this report, we show that the extracellular region of CD248 directly interacts with the IR, thereby dampening binding affinity of insulin to the receptor, interfering with its insulin-triggered autophosphorylation, and reducing downstream insulin-mediated activation of key substrates. This leads to adverse effects on glucometabolic function and lipid metabolism. The findings uncover a previously unrecognized molecular explanation for insulin resistance and thus a potential therapeutic strategy to reverse/prevent insulin resistance.

Methods

Mice

Mice lacking *CD248* (KO) on a C57Bl6 background were previously generated and genotyped as described.[16] Heterozygous (CD248$^{+/−}$) mice were interbred to generate CD248$^{+/+}$ (WT) and KO littermates, which were used in all studies. Sexes and ages were matched in all studies. Experiments involving mice were approved by the Institutional Animal Care Committee of UBC. Mice were housed in the Centre for Disease Modeling at the University of British Columbia, which is a 12:12 light:dark cycled, temperature and humidity-controlled, specific pathogen-free animal facility and with ad libitum access to food and water. At 8–9 weeks of age, mice were fed either a high-fat diet (HFD, D12492, 60% fat caloric content, Research Diets, New Brunswick, NJ, USA) or a normal chow diet (NCD, 2918, 18% fat caloric content, Harland Laboratories, Madison, WI, USA) for 2 weeks, after which they were either fasted or allowed continued access to food for 5 h. The animals were then euthanized with an anaesthetic overdose. Experiments were performed by personnel blinded to the genotype. The fat, muscle and liver were immediately removed, and blood was collected in tubes containing EDTA or Na-Citrate (final concentration of 0.2% and 3.2% of blood, respectively) via cardiac puncture of the right ventricle. Plasma insulin levels were quantified by enzyme-linked immunosorbent assay (mouse Insulin ELISA Kit, Mercodia, Uppsala, Sweden), according to the manufacturer's instructions. Excised tissues were either immersed in liquid nitrogen and kept frozen at −80 °C for future processing of the whole tissue or alternatively, processed immediately for glucose uptake and lipolysis assays, or the isolation of stroma vascular fraction (SVF) cells and preparation of preadipocytes.

Proteins and antibodies

Details of proteins and antibodies are provided in Supplemental Tables S1 and S2. All antibodies used were validated, as evidence by cited references.

Hyperinsulinemic-euglycemic clamp experiments

Hyperinsulinemic-euglycemic clamp experiments ("insulin clamps") were conducted in a cohort of mice to assess the role of CD248 in whole-body and WAT-specific insulin sensitivity and glucose utilization *in vivo*. Surgical and experimental protocols for mice undergoing insulin clamps were approved by the Animal Use and Care Committee at the University of Alberta. Anesthetized male mice (ketamine 90 mg/kg and 10 xylazine mg/kg), randomly ordered from the 2 genotypes, underwent vascular catheterizations following aseptic techniques to allow for intravenous infusions and blood sampling. Insulin clamp experiments were performed approximately 6 days after surgery when mice resumed pre-surgical daily food consumption amounts and were at least 90% of their presurgical body weight. Mice were fasted for 5 h prior to the start of experiments. A primed, intravenous infusion of [3-³H]-glucose (2 µCi bolus + 0.1 µCi/min; NET331C, PerkinElmer, Boston, MA, USA) was started at t = 0 min and maintained for the duration of the experiment to measure glucose kinetics. The basal period was defined as t = 40–60 min, inclusive. At

t = 60 min, a primed insulin infusion (2.0 mU/kg/min; Sigma I1553) was initiated with a concurrent variable infusion of glucose solution to maintain euglycemia. Plasma glucose concentrations were measured every 10 min for the duration of the clamp using a glucose analyzer (GM9, Analox Technologies North America, Toronto, ON, Canada). The clamp period was defined as t = 150–180 min, inclusive. To measure WAT-specific glucose utilization during hyperinsulinemia, a bolus of 2-[^{14}C]-deoxyglucose (12 µCi; NEC720A, PerkinElmer) was then intravenously injected at t = 180. Mice were anesthetized and euthanized 35 min after 14C-deoxy-glucose injection. Epididymal (e)WAT and quadriceps muscle samples were collected and immediately flash frozen in liquid nitrogen and stored at –80 °C until analysis. Plasma [3-^{3}H]-glucose and 2-[^{14}C]-deoxyglucose radioactivity were measured from deproteinized samples via liquid scintillation counting. Plasma insulin levels were taken from blood samples obtained just prior to t = 0 min and during the clamp period were measured using ELISA (80-INSMS, ALPCO, Salem, NH, USA). Tissue 2-[^{14}C]-deoxyglucose and 2-[^{14}C]-deoxyglucose-phosphate radioactivity were determined from supernatants of centrifuged tissues samples homogenized in 0.5% perchloric acid and neutralized with 5 N potassium hydroxide solution and normalized to tissue weight.

Isolation and culture of primary murine pre/adipocytes

Preadipocytes derived from WT and KO mice were isolated and validated as to their origin, as previously described with slight modifications.[27] Briefly, freshly excised eWAT from non-fasted mice was weighed, washed, minced and incubated with 0.2% collagenase type I in working solution (20 mM HEPES, 5 mM KH$_2$PO$_4$, 1 mM MgSO$_4$, 1 mM CaCl$_2$, 136 mM NaCl, 4.7 mM KCl, 209 µM adenosine power, 2% BSA, pH 7.4) at 37 °C in a shaking water bath for 45 min. The reaction was stopped by adding 3 volumes of working solution to the digested fat tissue, followed by passage through 100 µm and 70 µm cell strainers, followed by centrifugation. The floating mature adipocytes were aspirated, washed twice with sterile PBS, centrifuged at 500g at 4 °C and lysed for RNA extraction using the RNeasy Mini kit (Qiagen, Mississauga, ON, Canada). The pellet representing the SVF was resuspended in DMEM/F12. Cells were filtered, centrifuged, resuspended in growth media and counted. The Adipose Tissue Progenitor Isolation kit (Miltenyi Biotec, San Diego, CA, USA) was used to isolate the adipocyte progenitor cells from non-adipogenic cells according to the manufacturer's instructions. Briefly, the cell suspension was centrifuged at 300g for 5 min, and the supernatant was aspirated. Cells were resuspended, filtered and then incubated with the provided Non-adipocyte Progenitor Depletion cocktail for 15 min at 4 °C. The total reaction volume was adjusted to 500 µL, and the cell suspension was applied to a pretreated LS Column placed in the MACS Separator. Flow-through unlabeled cells were collected and incubated with Isolation Cocktail at 4 °C in the dark for 15 min and applied to a MS Column. After being washed, the remaining cells representing adipocyte progenitors, were flushed from the MS Column. Cells were grown in T75 cell culture flasks in complete medium (DMEM/f12 high glucose medium supplemented with 10% FBS, 100 U/mL penicillin and 100 g/ml streptomycin), at 37 °C in 5% CO$_2$. At 75% confluence, the adipocyte progenitor cells (pre-adipocytes) were treated with 0.25% Trypsin-EDTA and sub-cultured for experimental use at passages 2 to 3.

Quantitative qRT-PCR to measure CD248 transcripts

The qScript cDNA synthesis kit (Quanta Biosciences, Gaithersburg, MD, USA) was used to generate cDNA from isolated RNA. Relative transcript levels were analyzed using the StepOnePlus Real-Time PCR System (Applied Biosystems, Carlsbad, CA, USA) and Custom pre-designed primers (Taqman® Gene Expression Assays, ThermoFisher Scientific) for the genes of interest, CD248 (mouse Cd248 primer, Mm00547485_s1 Taqman gene expression assays) and the housekeeping gene GAPDH (mouse Gapdh primer, Mm99999915_g1 Taqman gene expression assays). Gene expression levels were normalized to GAPDH from the same sample. All experiments were performed in triplicate.

Isolation and culture of murine embryonic fibroblasts (MEFs)

MEFs were isolated from 12.5 to 13.5 day old male WT and KO murine fetuses as previously described.[28] Briefly, fetuses were dissected, internal organs were removed, and the remaining tissues were finely minced in 10 ml of sterile PBS. The minced tissue was subjected to two consecutive digestions in 0.25% trypsin-EDTA for 5 min at 37 °C, with the trypsin subsequently inactivated in Dulbecco's Modified Eagle Medium (DMEM) with 10% FBS. Digested tissue was plated onto 150 mm culture dishes, and adherent cells maintained in MEF basal media, consisting of DMEM (Life Technologies, Carlsbad, CA) with 25 mM glucose supplemented with 10% FBS, 2 mM L-glutamine, 1 mM sodium pyruvate and 100 U/ml penicillin-streptomycin. Cells were passaged when 80% confluent, and used for experiments between passage 2 and 5. The genotypes of the MEFs were confirmed.[16] As previously reported, expression of CD248 protein and RNA by MEFs from WT embryos and not from KO embryos, was confirmed by immunofluorescent staining, Western blot, and qRT-PCR.[16]

Human adipose tissue donors

Human abdominal subcutaneous adipose tissue biopsies were obtained from 10 subjects (9 women/1 man, BMI 30.5 ± 7.9 kg/m^2, age 51 ± 16 yo). Participant clinical and biochemical information are detailed in Supplemental Table S3. Subjects were fasted overnight and adipose tissue biopsies were performed by needle aspiration from the lower part of the abdomen after local dermal anesthesia with lidocaine (Xylocaine; AstraZeneca; Södertälje, Sweden). Subjects with diabetes, other endocrine disorders, systemic illness, and malignancy, as well as ongoing medication with immune-modulating therapies and glucocorticoids, were excluded from the study.

Human adipocyte isolation

Human adipocytes were isolated as previously described.[29] In brief, subcutaneous adipose tissue was digested in collagenase solution (1.0 mg/ml, from *Clostridium histolyticum*, Roche, Manheim, Germany) in Hank's medium (Medium 199, Gibco, Life Technologies, Paisley, UK) supplemented with 5.6 mM glucose, 4% bovine serum albumin (BSA, Sigma, MO, USA), 150 nM adenosine, pH 7.4, in a shaking water bath at 37 °C and 105 RPM. Following digestion with collagenase, the tissue was filtered through a nylon mesh and mature adipocytes were isolated, washed 4 times, and suspended in Hank's medium.

Human adipocyte lysates and immunoblotting

Isolated adipocytes were stimulated with or without a maximal insulin concentration (1000 µU/mL, 6 nM) for 15 min to prepare lysates, as previously described.[30] In brief, following incubation, the cells were separated from the medium and lysed at 4 °C for 2 h in lysis buffer (25 mM Tris-HCl, 0.5 mM EGTA, 25 mM NaCl, 1% Nonidet P-40, 1 mM Na$_3$VO$_4$, 10 mM NaF (all from Sigma), 100 nM okadaic acid (Alexis Biochemicals, Lausen, Switzerland), 1X Complete protease inhibitor cocktail (Roche, Indianapolis, IN, USA), and pH 7.4). Following centrifugation at 12,000 g, 15 min at 4 °C, the lysate was collected and the protein concentration was determined using a BCA protein assay kit (Pierce, Thermo Scientific, Rockford, IL, USA). Protein lysates (15 µg) were separated by SDS-PAGE (5–8% gradient, BioRad), transferred to nitrocellulose membranes, and blocked with 0.05% tween-phosphate buffer saline with 5% BSA. Membranes were incubated overnight in the solution of the primary antibodies: anti-CD248 (1:1000 Proteintech 60170-1-Ig), phospho-S473 AKT (1:1000, Cell Signaling 9271S), and total AKT (1:1000, Cell Signaling 9272S). Stain-free blot imaging was used to quantify the total protein for each sample and used to normalize total protein levels. Membranes were then washed with PBST and incubated with appropriate horseradish peroxidase-conjugated anti-rabbit and anti-mouse (Cell Signaling Technologies) secondary antibodies. Protein bands were visualized using enhanced chemiluminescence with a high-resolution field and quantified with ChemiDocTM MP System (BioRad).

Glucose uptake analyses

Glucose uptake in tissues was measured using a fluorescent D-glucose analogue 2-[N-(7-nitrobenz-2-oxa-1,3-diazol-4-yl) amino]-2-deoxy-D-glucose (2-NBDG, Invitrogen, OR, USA) by methods previously described with slight modifications.[31] Briefly, following euthanasia, fat explants, liver and gastrocnemius muscle were quickly excised. For WAT, sections were prepared with the mouse brain slicer (Zivic Instruments, PA) and washed with PBS. Liver and muscle homogenates were prepared with the Micro Tissue Homogenizer (Argos Technologies, Illinois, USA). Samples were incubated with serum- and glucose-free DMEM for 1 h at 37 °C, 5% CO$_2$ to deplete endogenous glucose stores. Subsequently, tissues were treated with insulin 800 nM or vehicle and 200 µM of 2-NBDG for 1 h. In pilot studies, the inclusion of 20 µM cytochalasin B, a specific inhibitor of GLUT proteins, revealed that nonspecific passive glucose uptake was negligible. After exposure to 2-NBDG, fat tissue slices were washed three times with serum- and glucose-free DMEM and counterstained with Hoechst 33,342 (Invitrogen, Molecular Porbes). Fluorescent images (×20 magnification) were detected by laser-scanning confocal microscopy (Eclipse Ti, Nikon, Tokyo, Japan) and quantified using ImageJ software (NIH, Bethesda, MD, USA), with the negative background chosen for the threshold setting. 2-NBDG uptake in liver and muscle tissues was measured using a microplate reader (SPECTRA max Plus, Molecular Devices) with excitation-emission detection of 465 nm$_{ex}$ and 540 nm$_{emiss}$, respectively.

Tissue lipid and glycogen analyses

Lipolysis in eWAT, inguinal white adipocyte tissue (iWAT), and retroperitoneal white adipocyte tissue (rWAT) was measured via glycerol release using the Free Glycerol Assay Kit (MAK117-1 KT, Sigma–Aldrich, St. Louis, MO, USA). Briefly, fat explants were incubated at 37 °C in 5% CO$_2$ for 2 h in KRH buffer (pH 7.4) with 2% albumin and fraction V fatty acids, and stimulated with 1 mM isoproterenol for 3 h. The release of glycerol was normalized to total protein levels. Triglycerides and glycogen were measured using the triglyceride quantification kit and glycogen assay kit II, respectively, from Abcam (Cambridge, UK) according to the manufacturer's instructions.

Preparation of recombinant purified proteins

Recombinant soluble forms of human thrombomodulin (TM) that comprise either the lectin-like domain (TMD1) or the entire extramembranous region (TMD1-3), and soluble CD248 that comprise the entire

extramembranous region (sCD248), were expressed in human embryonic kidney (HEK)293 cells and prepared and characterized as previously reported.[32,33] Recombinant functionally intact human insulin receptor (IR) was expressed in HEK293 T cells and purified as described.[34] IR preparations were kept on ice and used within 6 weeks.

Phosphorylation of the insulin receptor
Insulin induced phosphorylation of recombinant human insulin receptor (IR) was performed as previously reported with minor modifications.[34] Reactions containing 3.3 nM of the purified recombinant IR were incubated with 3.3–33 nM of soluble fragments of thrombomodulin (TMD1, TMD1-3) or sCD248 in buffer C (20 mM Tris, pH 8, 200 mM NaCl, and 0.03% DDM (n-Dodecyl-β-D-maltoside)). After a 20 min incubation at room temperature, 50–200 nM of insulin was added for 10 min at room temperature. Phosphorylation reactions were then initiated by the addition of 10X Kinase Buffer A (10 mM ATP, 10 mM $MgCl_2$ in buffer C). Reactions were stopped at different time points by removing equal volume aliquots and placing them immediately on ice into 5X Laemmli buffer. At the end of the experiment, equal quantities were separated by SDS-PAGE and Western immunoblotting was performed to detect total IR (rabbit anti-IRβ, Cat #3020S, Cell Signaling Technology, Beverly MA) and phosphorylated IR using antibodies that specifically detect phosphotyrosines 1161/1162 of the human IR (rabbit anti-insulin receptor (pTyr$^{1162/1163}$), EMD Millipore Cat#407707).

SDS-PAGE and western immunoblotting
Fat tissues (eWAT, iWAT and rWAT) were surgically excised from mice, frozen in liquid nitrogen, pulverized, and homogenized in RIPA buffer (30 mM Tris-HCl, 15 mM NaCl, 1% Igepal, 0.5% deoxycholate, 2 mM EDTA, 0.1% SDS) containing protease and phosphatase Inhibitor Cocktail (HALT, ThermoFisher Scientific, MA, USA). The homogenates were centrifuged at 4 °C for 15 min at 18,000 g, after which the supernatant lysates were collected and the protein concentrations were determined using the BCA kit (ThermoFisher Scientific, MA, USA). Equal amounts of protein (30–50 μg) were loaded and separated under reducing or non-reducing conditions by SDS-PAGE using 4–20% precast gradient gels (Protean TGX, Bio-Rad) and wet transferred onto nitrocellulose membrane for 2 h at 100V or at 4 °C overnight at 30V. Membranes were incubated for 1 h at room temperature with TBST (200 mM Tris, 1500 mM NaCl and 0.05% Tween-20, pH 7.4) containing 5% skimmed milk or 2% BSA, followed by incubation with primary antibodies at 4 °C overnight. After three washes with TBST, membranes were incubated with the appropriate secondary antibodies (100 ng/ml IRDye® 800 goat anti-rabbit or IRDye® 680 donkey anti-mouse, Licor, Nebraska, USA) diluted in blocking

buffer for 1 h at room temperature. Detection was accomplished using a Licor Odyssey® imaging system (Licor, Nebraska, USA). Protein bands were processed using ImageJ software (NIH, Bethesda, MD, USA). Relative protein expression was obtained via normalization with the corresponding total protein (for phosphorylated proteins) or with β-actin or GAPDH. All experiments were performed a minimum of 3 times, using fat isolated from different mice of the same age and sex, as noted.

Insulin binding studies
Recombinant human insulin (Sigma, St. Louis, MO, USA) was labeled with NHS-biotin using the EZ-Link NHS-Biotin kit (Thermo Fisher Scientific, Waltham, MA, USA) following the manufacturer's instructions. Free biotin was removed by dialysis, and the concentration of the remaining biotinylated insulin was quantified with the BCA kit. Purified SVF cells derived from the eWAT of WT and KO mice were seeded at a density of 20×10^3 cells per well in 96-well plates. After two days of culture, the cells were washed and equilibrated with serum-free and low glucose medium for 30 min at 37 °C, 5% CO_2. Cells were counted again to ensure equal numbers for each genotype. Cells were incubated at different intervals up to 120 min at 37 °C with 50 ng of biotinylated insulin. Nonspecific binding of biotinylated insulin was determined by performing the binding reaction in the presence of a 100-fold molar excess of unlabeled insulin. At the different intervals, cells were washed, fixed with 3.5% paraformaldehyde for 10 min, blocked with 2% BSA for 1 h, and then stained with Streptavidin DyLight 680 Conjugate (Rockland) secondary reagent for 1 h at room temperature and counterstained with Hoechst 33,342 (Invitrogen, Molecular Porbes) for 5 min at room temperature. Cells were imaged (×20 magnification) by laser-scanning confocal microscopy (Eclipse Ti, Nikon, Tokyo, Japan) and signals were quantified. Specific binding of biotinylated insulin to the cell surface was determined by subtracting the non-specific signal at each time point. Following determination of the time to achieve equilibrium binding, the above studies were repeated with an incubation time of 90′ with increasing concentrations of biotinylated insulin in the presence/absence of molar excess of unbiotinylated insulin. Specific binding curves were generated, and K_D values were calculated.[35] All experiments were performed in quintuplicate, and results shown represent the mean of 5 experiments.

Proximity ligation assay (PLA)
To test whether epitopes of two proteins were located close to each other (<40 nm), the *in situ* proximity ligation assay (PLA) was performed using the Duolink PLA Kit (Millipore Sigma).[22,23] Briefly, preadipocytes were cultured to preconfluence, fixed with cold methanol for

5 min, washed in PBS and incubated with the Duolink blocking solution for 30 min at 37 °C. Cells were further incubated for 30 min with a pair of antibodies (mouse anti-CD248 antibody (Proteintech, Chicago, IL, USA) and rabbit anti-insulin receptor β (IRβ) antibodies (E9L5V, Cell Signaling, MA, US)), each at 2 μg/ml. Controls included corresponding non-specific antibodies of the same species and isotype. After washes, the appropriate PLA probe Mix 1:40 was incubated for 1 h, followed by washes and addition of 25 μl of ligase for 30 min. Amplification was achieved by the addition of the DNA polymerase at 1:80 dilution for 100 min at 37 °C in the corresponding buffer. Slides were then mounted with DAPI for fluorescent imaging. Quantification was achieved by counting the number of fluorescent dots by ImageJ software set for a fixed area (magnification 60× objective), in a minimum of 7–10 random fields of interest per condition (n ≥ 3 experiments per condition). Fluorescence intensity was quantified with NIH ImageJ 1.50i imaging software (NIH, Bethesda, MD, USA).

Co-immunoprecipitation of CD248 with the IR
Cultured cells were washed with PBS at 4 °C and then lysed in ice-cold RIPA buffer (50 mM Tris HCl, 150 mM NaCl, 2 mM EDTA, 0.35% NP-40, 0.5% sodium deoxycholate) containing protease and phosphatase Inhibitor Cocktail (HALT, ThermoFisher Scientific, MA, USA). Lysates were centrifuged at 18,000×g for 15 min, and protein concentrations of supernatants were determined using a BCA kit and adjusted to 100–200 μg/μL. Samples were incubated with 1 μg of mouse anti-IRβ (9L55B10, Cell Signaling, MA, USA) or mouse anti-CD248 (Proteintech, Chicago, IL, USA) for 3 h at 4 °C, followed by incubation with 25 μL of protein A/G PLUS-Agarose (Santa Cruz Biotech cat sc-2003) for 1 h at 4 °C. The beads were washed five times with RIPA, suspended in Laemmli buffer, and heated x 5 min at 95 °C in preparation for SDS-PAGE and Western immunoblotting to detect CD248 and the IR.

Co-immunoprecipitation of CD248 with integrin β1
Co-immunoprecipitation experiments were performed using antibodies crosslinked to magnetic Dynabeads Protein G (ThermoFisher Scientific, MA, USA), separated with a DynaMag-2 magnet (ThermoFisher). For each reaction, 1.5 mg of beads was incubated with 5 μg of either anti-CD248 antibody or anti-integrin β1 (clone MB1.2, Merck Millipore) for 10 min at room temperature. Beads were washed with PBS prior to performing a crosslinking reaction using 5 mM bis(sulfosuccinimidyl)suberate (BS3, ThermoFisher Scientific) for 30 min at room temperature. The reaction was quenched with 1 M Tris HCl (pH 7.5) and washed with 0.02% PBS-Tween (PBST) to remove unbound antibody. Beads were then added to cell lysates (normalized to 300 μg total protein per reaction, diluted in 0.02% PBST)

and incubated overnight at 4 °C. After multiple washes, immunoprecipitates were eluted with 20 μL of 10% sodium dodecyl sulfate (SDS) prior to analysis by SDS-PAGE and Western blotting with specific antibodies to detect CD248 and integrin β1.

Ethics
Human studies were conducted in accordance with the most current Declaration of Helsinki and with approval of the Regional Ethics Review Board in Uppsala (Dnr2013-183/494, Dnr2018-385). Participation was voluntary with informed consent. Experimental animal procedures were approved by the Institutional Animal Care Committees of the University of British Columbia (CCAC A22-0159) and the University of Alberta (AUP00003818).

Statistical analyses
Statistical analyses were carried out using Graph Prism 8 (Graph Pad Software, San Diego, CA). The Kolmogorov–Smirnov test or D'Agostino–Pearson normality test was used to determine whether the data followed a Gaussian distribution. Differences between 2 groups were analysed by unpaired Student's t-test or Mann–Whitney as parametric and non-parametric tests, respectively. Differences between more groups were analysed using one-way ANOVA with *post hoc* comparisons made using Bonferroni's test. Data are presented as mean ± SEM. A p-value of <0.05 was considered significant.

Role of funders
No funding sources were involved in the writing of the manuscript or the decision to submit it for publication. No authors were paid to write this article from any source or agency. The corresponding authors had full access to all the data in the study and had final responsibility for the decision to submit for publication.

Results
We previously showed that global lack of *CD248* in mice (KO) confers protection of male mice against 9-weeks of a HFD that induced obesity, insulin resistance, glucose intolerance, steatosis, WAT hypoxia, inflammation and fibrosis.[18] For the current studies, we found that even exposure to 2 weeks of the HFD induced differences in glucometabolism between male KO mice and their wild-type (WT) counterparts (Supplemental Figures S1–S4). Thus, the KO mice had significantly lower fasting plasma insulin and insulin growth factor (IGF)-1 levels (Supplemental Figure S1) as compared to sibling control, sex matched HFD-fed WT mice, with significantly better responses in glucose tolerance and insulin tolerance tests (GTT & ITT, respectively) (Supplemental Figure S2).]Immunohistochemical analyses of epididymal (e)WAT from the HFD-fed KO mice followed by

fasting x 5 h, revealed less evidence of fibrosis, less infiltration with F480 inflammatory monocytes, and reduced hypoxia, as compared to fasting HFD-fed wild-type (WT) mice (Supplemental Figures S3 and S4). There was no evidence of steatosis in either group (not shown) following the 2 week HFD. Based on these findings, we used this 2-week HFD model to study the mechanisms by which CD248 regulates glucometabolism and insulin sensitivity.

Clamping studies

Our global and adipocyte-specific *CD248* gene inactivation studies[18] support the notion that CD248-dependent adipocyte insulin signaling impacts on whole body glucometabolic homeostasis. To quantify CD248-dependent insulin sensitivity in mice *in vivo*, we used the gold-standard hyperinsulinemic-euglycemic clamp with tracer dilution methodology ("insulin clamp") to assess glucose kinetics under basal and hyper-insulinemic conditions[36–38] (Fig. 1a). For each genotype, male mice were placed on a normal chow diet (NCD) until 8 weeks of age; then one subset was placed on the

HFD while the rest stayed on the NCD. As expected, HFD-feeding for 2 weeks rendered mice hyper-insulinemic (Table 1) prior to diet-induced changes in body weight (Table 1), and markedly decreased the requirement for exogenous glucose infusion during insulin clamp conditions (Fig. 1b). This corresponded with greater hepatic glucose production (Fig. 1c) and reduced insulin-stimulated glucose disposal (Fig. 1d) compared to normal chow diet (NCD)-fed mice. Thus, 2 weeks of HFD-feeding induces insulin resistance in mice, irrespective of genotype, prior to an increase in body weight gain.

However, following 2 weeks of HFD, the glucose infusion rate (GIR) during the insulin clamp was greater in KO mice compared to their WT counterparts (Fig. 1b). This increased requirement for exogenous glucose infusion in HFD-KO mice occurred in concert with lower hepatic glucose production (Fig. 1c) and an increased rate of whole-body insulin-stimulated glucose disposal (Fig. 1d) compared to HFD-WT mice. These changes occurred independently of changes in plasma glucose (Supplemental Figure S5a), plasma insulin
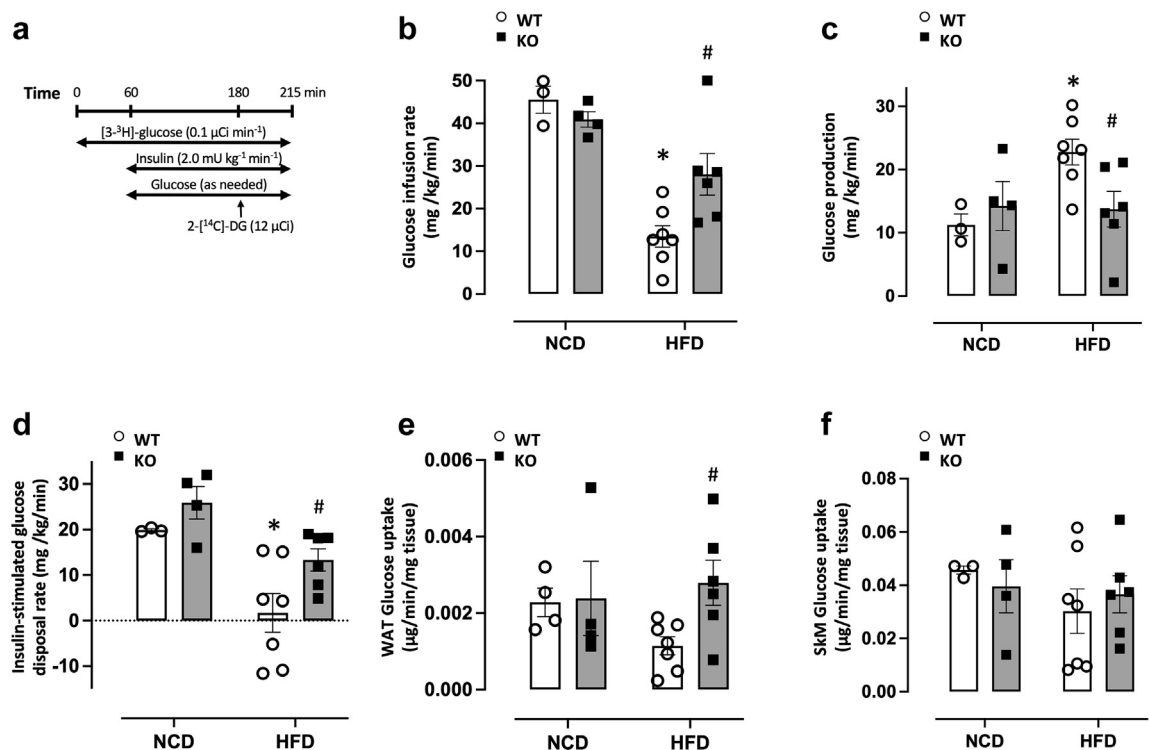
Fig. 1: Deletion of CD248 improves insulin sensitivity in high fat diet (HFD)-fed mice with increased insulin-stimulated glucose uptake in white adipose tissue, in vivo. (a) Hyperinsulinemic-euglycemic clamp experiment study design. (b) Glucose infusion rates; (c) hepatic glucose production rates; and (d) insulin-stimulated glucose disposal rates (calculated as the difference between the glucose utilization rate and rate of basal glucose production) during the clamp period in wildtype (WT; n = 3, n = 7) and KO (n = 4, n = 6) mice fed with normal chow diet (NCD) or HFD, respectively. *In vivo* glucose uptake rates in: (e) white adipose tissue (epididymal) and (f) skeletal muscle (SkM; quadriceps) during the final 35 min of the insulin clamps following intravenous 2-[^{14}C]-deoxyglucose (DG) injection. *p < 0.05 HFD WT *vs* NCD WT; #p < 0.05 HFD KO *vs* HFD WT (1-way ANOVA).

	NCD WT	NCD KO	HFD WT	HFD KO
	(n = 3)	(n = 4)	(n = 7)	(n = 6)
Body Weight (g)	28.6 ± 1.2	27.0 ± 1.6	30.9 ± 2.4	32.4 ± 1.0
Pre-clamp				
Insulin (ng/ml)	0.71 ± 0.21	0.84 ± 0.12	1.67 ± 0.32[a]	1.55 ± 0.15
Clamp				
Insulin (ng/ml)	1.01 ± 0.04	1.16 ± 0.25	2.09 ± 0.48	2.54 ± 0.41

[a]$p < 0.05$ vs NCD WT (1-way ANOVA).

Table 1: Body weight and plasma insulin levels before ("pre-clamp") and during the clamp period in mice that underwent hyperinsulinemic-euglycemic clamp experiments.

levels (Table 1) and body weight (Table 1). Basal glucose production was also similar in both groups (Supplemental Figure S5b). In NCD-fed mice, CD248 deficiency did not affect glucose kinetics in mildly hyperinsulinemic conditions *in vivo*.

To assess whether improved peripheral insulin sensitivity was due to an enhancement of insulin-stimulated glucose uptake *in vivo*, we measured glucose uptake in WAT and skeletal muscle during the insulin clamp using 2-[^{14}C]-deoxyglucose. The increased rate of insulin-stimulated glucose disposal in HFD-fed KO mice compared to HFD-fed WT mice was associated with an increased rate of glucose uptake in WAT (Fig. 1e), without effects on skeletal muscle glucose uptake (Fig. 1f). Taken together, these data suggest that a lack of CD248 improves glucose metabolism *in vivo* by enhancing insulin sensitivity in the liver to suppress glucose production, and in the WAT (but not in skeletal muscle) to stimulate glucose uptake in diet-induced insulin resistant mice.

Lack of CD248 displays improved glucose metabolism and increases WAT insulin sensitivity

Complementing the insulin clamp studies, two approaches were used to examine the role of CD248 in modulating insulin-triggered glucose uptake into tissue explants. In the first, following 2 weeks of a NCD or HFD in male WT and KO mice, WAT from different depots was surgically excised and the explants were immediately sliced and placed into media, whereupon they were incubated with or without insulin in the presence of the fluorescent D-glucose analogue, 2-NBDG. In the absence of insulin, eWAT from the NCD-fed KO mice displayed a significantly increased uptake of 2-NBDG compared to NC-fed WT animals (Fig. 2a and b). This difference was markedly enhanced when the eWAT explants were exposed to insulin *ex vivo*. The HFD partly dampened the uptake of 2-NBDG under all conditions, such that there were no detectable differences in baseline glucose uptake in eWAT from HFD-fed KO *vs* HFD-fed-WT mice. However, glucose uptake of insulin-stimulated eWAT from HFD-fed KO mice was significantly greater as compared

to uptake in eWAT from HFD-fed WT mice. The data are consistent with the *in vivo* insulin clamp studies, indicating that lack of CD248 renders the mice more responsive to insulin-mediated glucose uptake into WAT (Fig. 2a).

By a second approach, a similar assay was used to quantify the effect of CD248 expression on insulin-triggered glucose uptake. Explants of adipose tissues from WT and KO mice were minced, washed and incubated with 2-deoxyglucose (2DG), after which the intracellular phosphorylated form, 2-DG6P (36), was quantified by a colorimetric assay. Following the 2 week NCD, lack of CD248 resulted in a significant increase in basal glucose uptake (reflected by increased levels of 2-DG6P) in all 3 WAT depots tested (Fig. 3) Incubation of insulin with the WAT explants from the NCD-fed mice resulted in increases in glucose uptake, to a significantly greater extent in WAT from the KO mice from all three fat depots. Similarly, following a 2 week HFD, eWAT and inguinal (i)WAT from the KO mice responded to insulin incubation with a significantly greater uptake of glucose, with a lesser differential response in the rWAT (Fig. 3). As might be expected, since CD248 is not expressed by BAT,[18] we did not detect any genotype-dependent differences in glucose uptake in BAT derived from the mice.

We also evaluated whether CD248 impacts glucose homeostasis in the muscle (gastrocnemius) and liver of mice following 2 weeks of the NCD or HFD. Although insulin incubation with these explanted tissues resulted in an increase in glucose uptake measured by 2-NBDG fluorescence, there were no significant CD248-dependent differences in uptake (Supplemental Figure S6a and b), findings that were consistent with the *in vivo* insulin clamp studies. Glycogen stores in the livers of the KO mice, following either the NCD or the HFD, were slightly increased (Supplemental Figure S6c), but not to a significant extent, as compared with livers of corresponding WT mice.

Lipolysis in WAT is dampened in absence of CD248

CD248-dependent changes in lipolysis were tested in WAT explants by measuring the secretion of glycerol

a

b
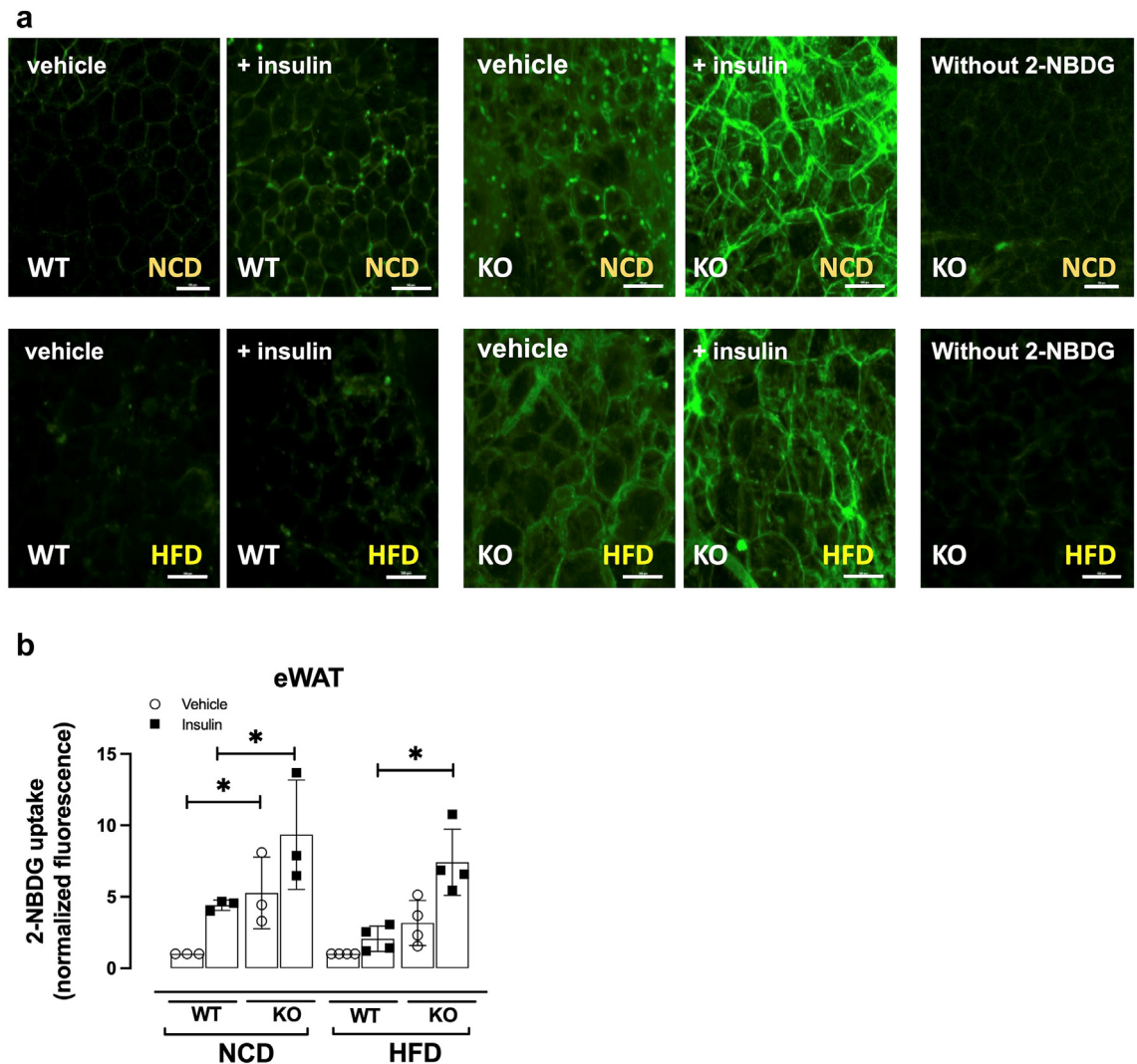
Fig. 2: **Glucose uptake in epididymal WAT (eWAT) explants from** *CD248* **wild-type (WT) and knockout (KO) male mice**. (**a**) Representative images of glucose uptake in epididymal eWAT explants from WT and KO mice fed a normal chow diet (NCD) or a high-fat diet (HFD) for 2 weeks. Explants were incubated with or without insulin and the fluorescent D-glucose analog, 2-NBDG. Fluorescence intensity (green) indicates glucose uptake, with higher intensity representing increased uptake. Images were observed via laser scanning confocal microscopy at 20× optical magnification. Size bar 100 μm. (**b**) Quantitative analysis of fluorescence intensity in panel A for glucose uptake. *$p < 0.05$. Results are expressed as the mean ± SEM (1-way ANOVA).

under baseline conditions and in response to isoproterenol. Following a 2-week NCD, glycerol secretion from WAT explants from WT and KO mice was not different, all responding to isoproterenol with similar increases in secretion (Fig. 4a–c). In contrast, following a 2 week HFD, lack of CD248 resulted in significantly decreased glycerol release from eWAT, iWAT and retroperitoneal (r)WAT, as well as an almost total lack of response to the isoproterenol (Fig. 4a–c). This occurred in parallel with a significant increase in accumulation of triglycerides in the WAT (eWAT) of the HFD-fed KO mice (Fig. 4d), with slight, non-significant decreases in plasma and liver triglyceride levels in HFD-fed KO mice

as compared to HFD-fed WT mice (Fig. 4e and f). The findings are consistent with suppression of lipolysis in the HFD-fed KO mice.

WAT from KO mice exhibits enhanced activation of AKT phosphorylation-dependent pathways

Insulin controls the key metabolic activities of glucose uptake, glycogenesis, lipogenesis/lipolysis, protein synthesis and adipogenesis[5–7] by triggering intracellular signaling cascades that lead to cellular responses. Although multiple regulatory and accessory pathways are involved, 2 canonical pathways have been described, i.e., the Ras/MAPK pathway and the AKT-PI3 kinase
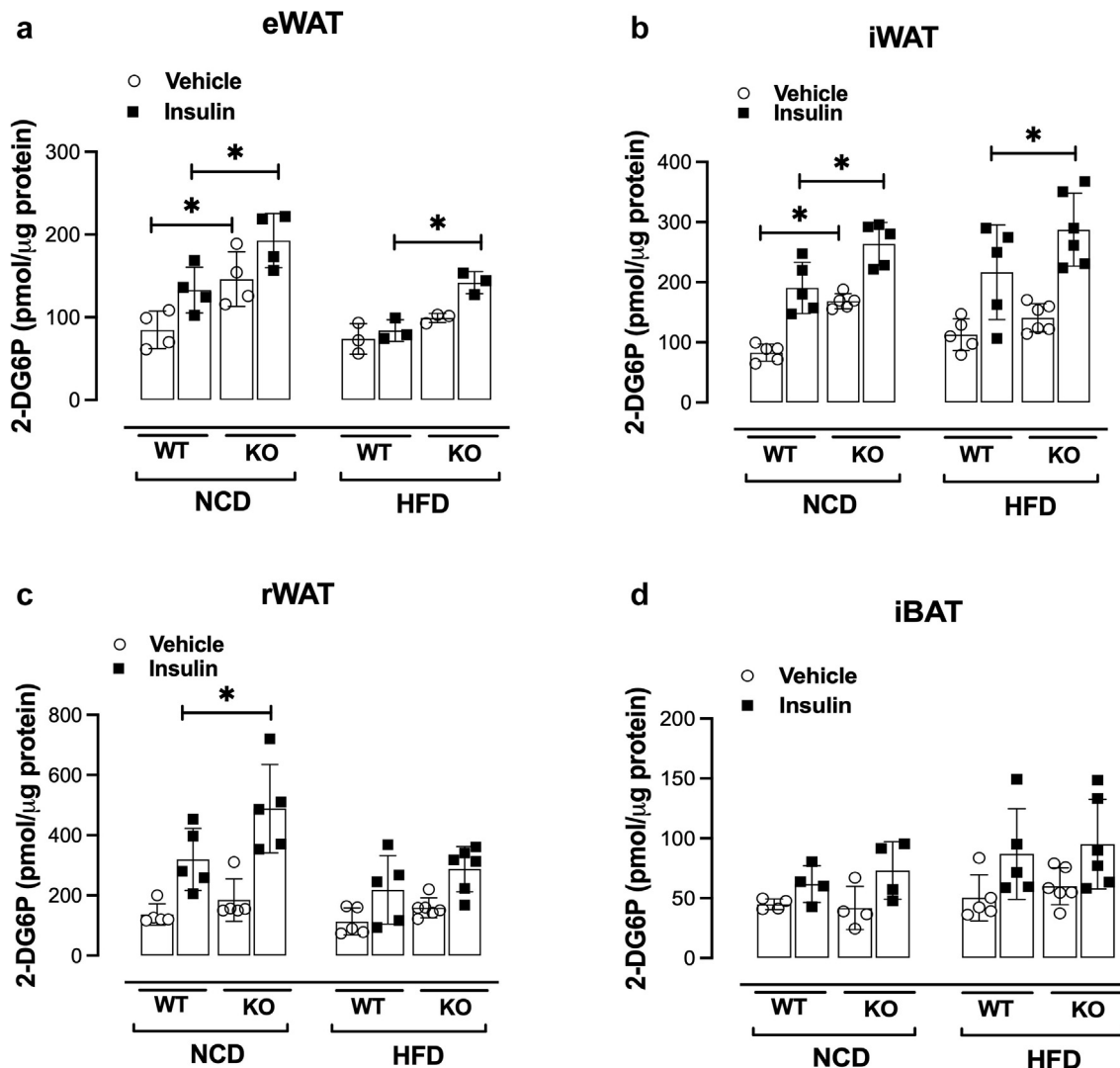
Fig. 3: Effect of CD248 expression on insulin-triggered glucose uptake in adipose tissue explants. Glucose uptake was quantified in minced explants of adipose tissues from WT and KO male mice fed a NCD or a HFD using the 2-deoxyglucose (2DG) assay. 2-DG uptake was determined under basal conditions and in response to insulin. 2-DG uptake was measured spectrometrically at an absorbance of 412 nm on a microplate reader in kinetic mode every 2–3 min at 37 °C. (**a**) epididymal WAT (eWAT) 2-DG uptake; (**b**) inguinal WAT (iWAT) 2-DG uptake; (**c**) retroperitoneal WAT (rWAT) 2-DG uptake; (**d**) interscapular BAT (iBAT) 2-DG uptake. *$p < 0.05$. Results are expressed as the mean ± SEM (1-way ANOVA).

(PI3K) pathway.[39] We examined the effects of CD248 expression on activation of these pathways in WAT lysates from WT and KO mice following a 2 week NCD or HFD and fasting for 5 h.

Following engagement and activation of insulin's cognate receptor and consequent activation/phosphorylation of intracellular substrates and proteins, activation of AKT requires that it become phosphorylated at 2 sites - serine 473 and threonine 308. Immunoblots of lysates of iWAT from KO mice revealed a significant increase in both pAKT^thr308 and pAKT^ser473 following a NCD and a HFD (Fig. 5a, c). This was also evident in eWAT, although the increase in pAKT^ser473 following the HFD

did not achieve statistical significance (Fig. 5b, d). There were no apparent changes in the levels of total AKT, irrespective of the diet or the genotype. We could also not ascribe any differences in AKT phosphorylation to CD248-dependent changes in expression of the IR, as the levels of IRβ by Western blot were not affected by the presence or absence of CD248 or by the diet (Supplemental Figure S7). Thus, lack of CD248 results in increased insulin-induced AKT phosphorylation in these WAT depots.

We next evaluated activation/phosphorylation of selected downstream AKT effectors that regulate WAT insulin sensitivity, glucose uptake and lipolysis.
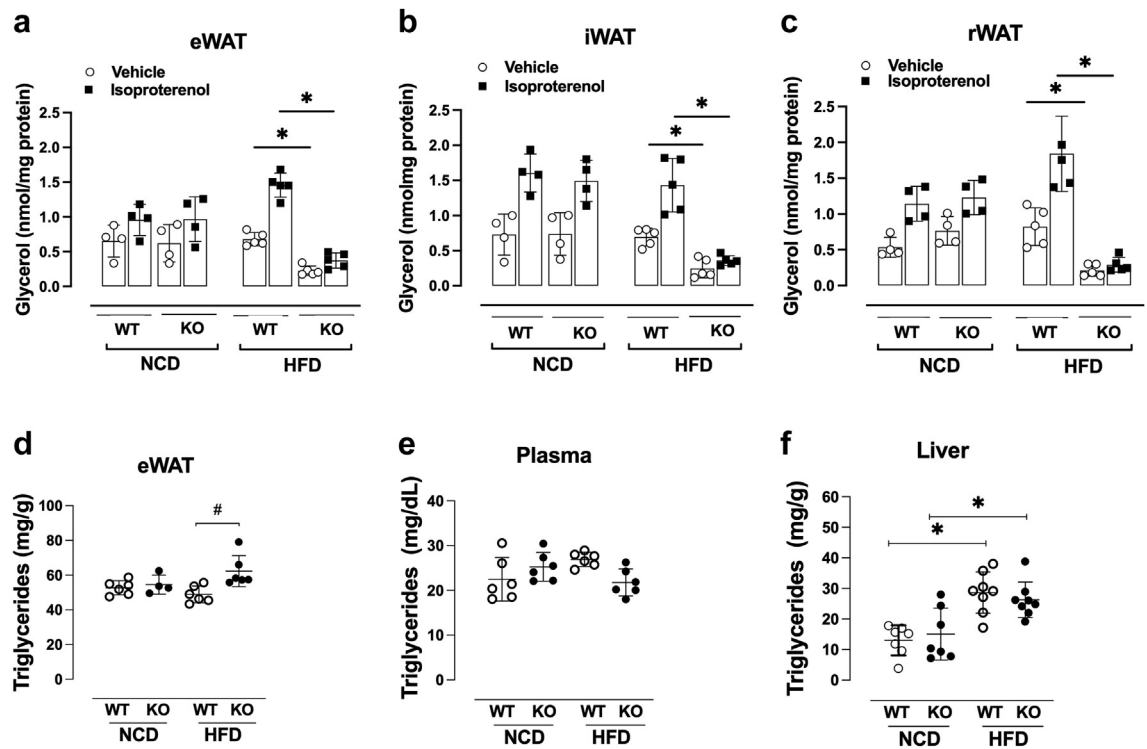
Fig. 4: **CD248 knockout impacts on lipid metabolism**. WT and KO male mice were fed a NCD or HFD for 2 weeks. Fat tissue samples were collected and placed in an incubator at 37 °C for hours. The fat tissue was then stimulated with 1 mM isoproterenol for 3 h. The amount of glycerol released during the experiment was adjusted based on the total protein levels. After 2 weeks of HFD, glycerol release from (**a**) eWAT, (**b**) iWAT and (**c**) rWAT from KO mice was significantly less compared to WT mice under basal and isoproterenol stimulated conditions. Triglycerides were measured in (**d**) eWAT, (**e**) plasma and (**f**) livers of mice. *$p < 0.05$. Results are expressed as the mean ± SEM (1-way ANOVA).

Glycogen synthase kinase (GSK)3 is a serine–threonine protein kinase, the beta form (GSK3β) of which can be directly phosphorylated at serine 9 and thus inactivated by AKT.[40] GSK3 has multiple functions in energy metabolism that may contribute to obesity, glucose intolerance and insulin resistance. In adipose tissue, GSK3 negatively regulates insulin signaling by phosphorylating and inactivating the IR and the insulin receptor substrate (IRS)-1.[40] In line with increased AKT phosphorylation in WAT from KO mice, GSK3β phosphorylation was increased in the lysates of both iWAT and eWAT from KO mice fed a NCD or a HFD diet (Fig. 5). No significant changes in the expression levels of total GSK3β were observed. The findings are again consistent with the observed increased insulin sensitivity in the KO mice.

Insulin-triggered activation and phosphorylation of threonine 389 on p70S6 is important in promoting glucose uptake, in part by upregulating expression of the membrane associated glucose transporter, GLUT4.[41] While total expression of p70S6 was unchanged (Fig. 5), expression levels of the phosphorylated form, p-p70S6[thr389] were significantly increased in the lysates of iWAT and eWAT of fasting male KO mice fed a HFD compared to male WT counterparts. This CD248-dependent effect on p-p70S6[thr389] was not evident when mice were fed a NCD. Nonetheless, GLUT4 expression was significantly increased in iWAT and eWAT of the fasted KO mice fed a NCD, and in eWAT of HFD-fed KO mice (Fig. 5). These findings are consistent with our *in vivo* insulin clamp studies and *ex vivo* explant glucose uptake experiments.

We also examined the effect of exogenous insulin on phosphorylation of selected insulin signaling targets (Supplemental Figure S8). To that end, WT and KO male mice were placed on a HFD x 2 weeks and fasted x 5 h prior to injection with insulin (2 IU/kg ip) or vehicle. After 30 min, eWAT was isolated for Western blot analyses. AKT phosphorylation (Ser473) was detectable in the absence of insulin, but notably increased in response to insulin. Consistent with our previous findings (Fig. 5), AKT phosphorylation (Ser473) in the lysates of eWAT from the HFD-fed KO mice, was elevated with vehicle-treatment. The addition of insulin had little further effect. A similar pattern of expression was noted for GLUT4. While we again found higher levels of p-p70S6 in the KO eWAT lysates as compared to those
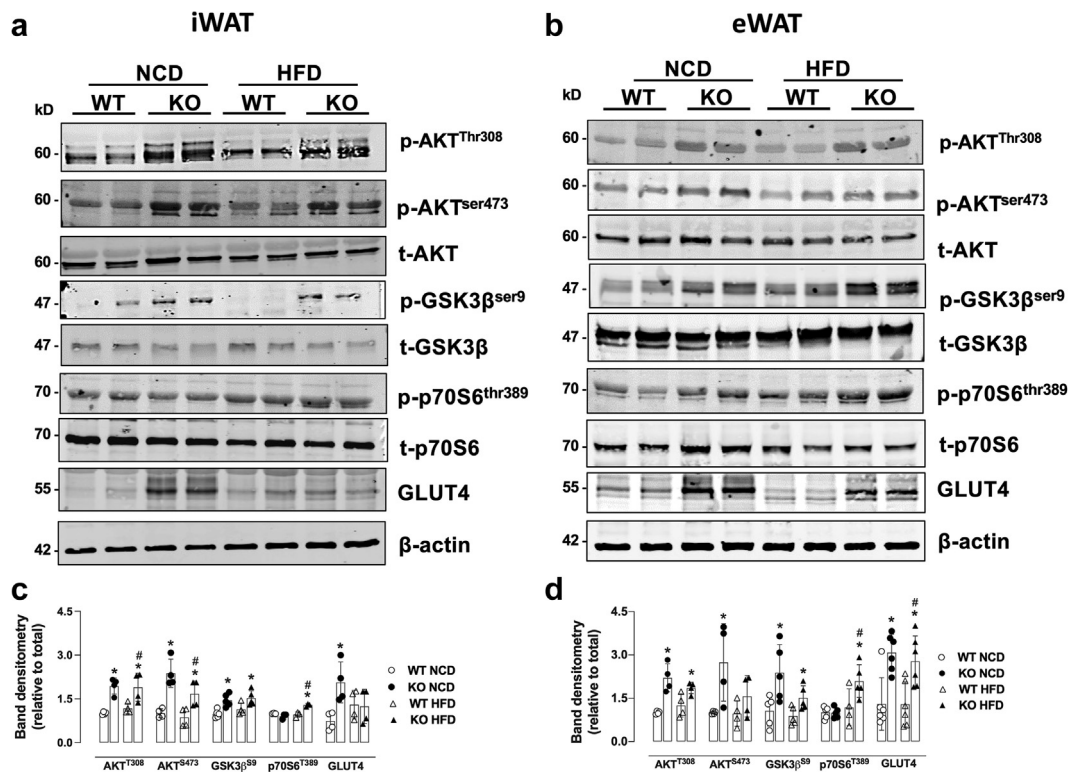
Fig. 5: AKT phosphorylation-dependent pathway analyses in WAT from mice. (**a, c**) iWAT and (**b, d**) eWAT was prepared from WT and KO male mice fed a NCD or HFD for 2 weeks followed by a 5 h fast. (**a-b**) WAT lysates were Western immunoblotted with the indicated antibodies, and protein levels were quantified by densitometry and normalized to corresponding total proteins or β-actin (**c-d**). *p < 0.05 *vs* WT-NCD group. #p < 0.05 *vs* WT-HFD group. Results are expressed as the mean ± SEM. n = 4–6 mice per group as noted (1-way ANOVA).

from WT eWAT, there was little response noted with insulin under these conditions.

To evaluate the effect of CD248 on key insulin-regulated intracellular pathways that regulate lipolysis we measured the levels of adipose triglyceride lipase (ATGL) and hormone-sensitive lipase (HSL)[42] (Fig. 6a and b). Consistent with the reduced lipolysis observed in the WAT explants from KO mice and increased triglyceride levels in the WAT of KO mice, ATGL expression was significantly decreased following the HFD in all 3 WAT depots from KO mice (Fig. 6a and b), whereas phosphorylated HSL (p-HSL^{Ser563})–absolute amounts or relative to total (t)-HSL–were either unchanged (iWAT) or slightly increased (eWAT, rWAT) (Fig. 6a, c).

Insulin-triggered activation of the Ras/Raf/MAPK pathway is often associated with the mitogenic and growth effects of insulin signaling. It is less well-established than the AKT/PI3K pathway in regulating adipose tissue function.[43] In limited studies in WAT lysates, we did not observe consistent CD248-dependent changes in phosphorylation of ERK1/2 or of Ras. Phosphorylated Raf (C-Raf$^{298/296/301}$, C-Raf^{259}) appeared to be moderately increased in the eWAT from KO mice,

particularly after 2 weeks of a NCD, but not to a significant extent (Supplemental Figure S7).

Role of sex in CD248-dependent effects on glucometabolism and insulin sensitivity

The preceding studies were all performed in male mice. In more limited experiments, we also examined female mice to assess for CD248-dependent changes in gluco-metabolism and insulin sensitivity. In female mice on a NCD, we did not detect CD248-dependent differences in the GTT or ITT (not shown). Following 2 weeks of a HFD, the WT and KO mice had similar responses in ITT (Supplemental Figure S9a, b). However, under these conditions, the GTT was significantly better in the KO *vs* the WT mice (Supplemental Figure S9c, d). With WAT explants from the HFD-fed female mice, baseline glucose uptake was modestly increased in KO eWAT (p < 0.05), and significantly increased in iWAT following insulin stimulation (Supplemental Figure S9e and f). Total expression of the IR (IRβ) was not notably affected by diet or the presence or absence of CD248 (Supplemental Figure S10a and b). AKT phosphorylation was increased, particularly in iWAT from HFD-fed
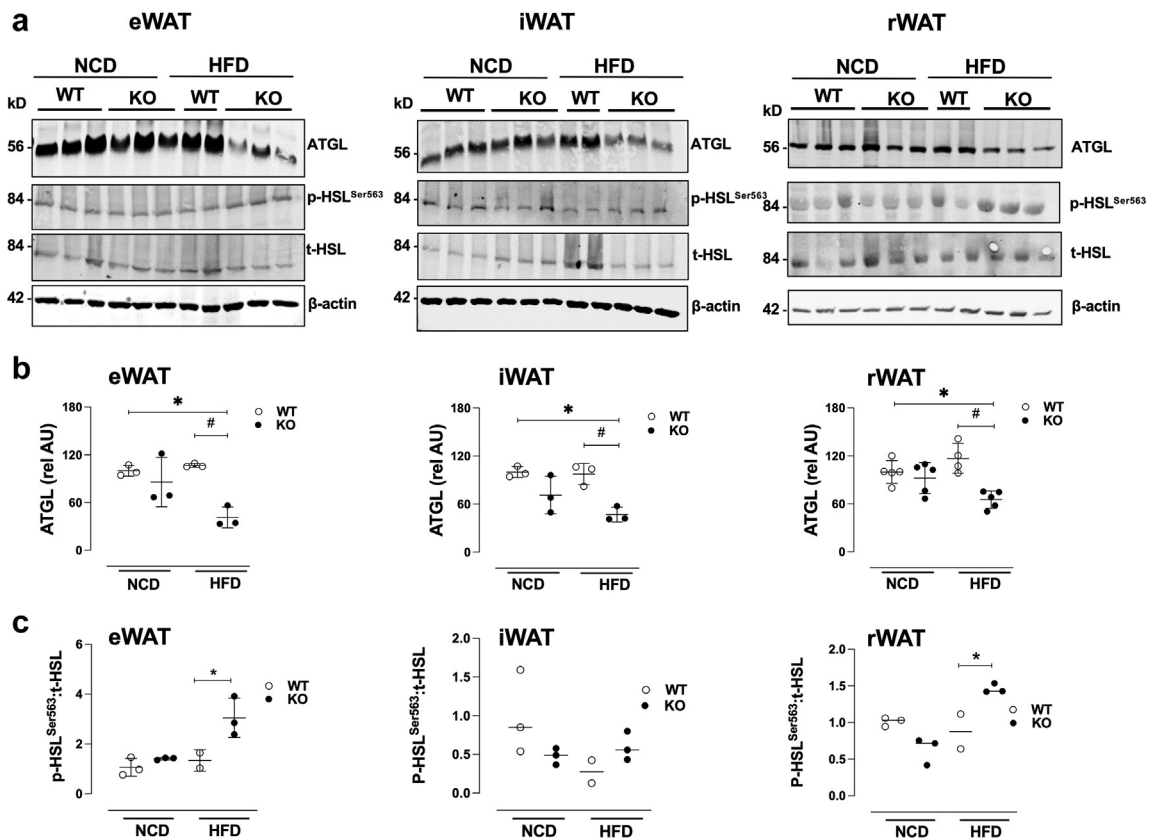
Fig. 6: **CD248-dependent changes in WAT fat pad lipases**. After 2 weeks of a NCD or HFD, fat explants (eWAT, iWAT and rWAT) were collected and processed for (**a**) Western blot analysis of ATGL, p-HSL^{Ser563} and t-HSL. (**b–c**) Densitometry was used to quantify protein expression of ATGL relative to β-actin, and p-HSL^{Ser563} relative to total HSL. *p < 0.05 *vs* WT-NCD group and #p < 0.05 *vs* WT-HFD group. Results are expressed as the mean ± SEM. n = 3–5 mice per group as noted (1-way ANOVA).

female KO mice, but this was not reliably observed in other WAT depots. Moreover, although GLUT4 was increased in eWAT from NCD-fed KO mice, it was not consistently increased under any other conditions or in other WAT depots. Overall, in response to a NCD or HFD, the adverse effects of CD248 on glucometabolism observed in male mice of the same age, were replicated in female mice, but to a much lesser extent.

Effect of diet and fasting on CD248 expression by mature adipocytes

We previously reported a strong direct correlation of *CD248* mRNA levels in mature adipocytes from subcutaneous WAT from humans with obesity and insulin resistance.[18] To test the effect of the diets on *CD248* expression in murine WAT, we measured the effects of a 2 week NCD and HFD, followed by fasting and non-fasting (5 h), on expression of *CD248* mRNA in mature adipocytes from eWAT and iWAT of male and female WT mice (Supplemental Figure S11). Consistent with our previous findings in humans,[18] *CD248* transcript levels were moderately higher in the adipocytes

from the HFD non-fasting mice, a finding more evident in eWAT than iWAT. While *CD248* transcript levels following the NCD were not affected by fasting, in both fat depots and with both sexes, fasting following the HFD resulted in a ~1.5-4-fold increase in adipocyte *CD248* mRNA levels.

CD248-dependent effects on insulin-signaling in preadipocytes

Adipose tissue comprises numerous cell types, several of which may express CD248. These include pre-adipocytes, mature adipocytes, perivascular cells and inflammatory leukocytes. We isolated preadipocytes from WAT of male and female WT and KO mice to assess their differential responses to insulin. Immuno-fluorescent staining of the cells for CD248 from WAT of WT and KO mice confirmed their genotype, the absence of apparent genotype-dependent morphologic or growth rate characteristics, the purity of the preparations, and the high expression of CD248 in the WT cells (Supplemental Figure S12). From Western blots (Supplemental Figure S13) and immunofluorescent

staining of the non-permeabilized cells (Supplemental Figure S12), preadipocytes from WT and KO cells expressed similar amounts of insulin receptor (IRα).

As expected, insulin induced phosphorylation of AKT in a time-dependent manner in preadipocytes purified from WT and KO mice (Supplemental Figure S13), notably more rapidly and to a greater extent in KO pre-adipocytes as compared to the WT preadipocytes. Again, like the WAT from KO mice, p-GSK3β[ser9] was increased in the KO preadipocytes (Supplemental Figure S13a). However, in contrast to the WAT findings, p-Erk1/2 was consistently increased in the KO preadipocytes, with responses similar in cells derived from male and female mice (Supplemental Figure S13).

We also evaluated insulin-dependent phosphorylation of adipocytes isolated from the subcutaneous WAT of a small cohort of obese human volunteers (Supplemental Table S3a). Adipocyte expression levels of CD248 were evaluated by Western blot, and divided into 2 groups, either "High CD248" or "Low CD248" (n = 5 per group). There were no significant differences in the groups of participants, in terms of age and BMI (Supplemental Table S3b). Consistent with what we observed with murine preadipocytes, human WAT adipocytes with lower levels of CD248, responded to insulin stimulation with greater increases in pAKT relative to total AKT (Supplemental Figure S14).

CD248 directly interacts with the insulin receptor

In view of the effects of CD248 on both canonical insulin signaling pathways in the preadipocytes, we considered the possibility that CD248 might directly modulate the interaction between insulin and the insulin receptor (IR). Proximity ligation assays using primary cultured preadipocytes from WT and KO mice confirmed that CD248 is indeed in close proximity to the IR (Fig. 7a). Non-specific signals were excluded using isotype-matched antibodies (NSIg) for each of the specific antibodies (anti-CD248 and anti-IRβ). No signal was detected when we used preadipocytes from WAT of KO mice. The interaction between CD248 and the IRβ was further confirmed by co-immunoprecipitation studies in which CD248 was pulled down with specific anti-CD248 antibodies, and the blots were immunodetected with anti-IRβ antibodies. Control experiments with non-specific antibodies (NSIg) did not pull down the IR (Fig. 7b and c).

In response to diet-induced reorganization of the extracellular matrix of adipose tissue, integrin activity reportedly regulates insulin sensitivity.[44] Since integrin β1 is one of few integral membrane proteins that interact directly with the IR on the outside of the cell membrane,[44] we explored the possibility that CD248 might also bind to integrin-β1 (ITGβ1). We used lysates of murine embryonic fibroblasts (MEFs) from WT and KO embryos and first showed that levels of ITGβ1 are not CD248-dependent. In co-immunoprecipitation

studies, we found that both anti-CD248 and anti-ITGβ1 antibodies pulled down CD248 and ITGβ1, indicating that these two proteins closely interact or bind to each other (Supplemental Figure S15a and b). Lysates from KO MEFs served as negative controls. Confocal imaging of WT MEFs, visually confirmed that CD248 colocalizes with ITGβ1 on the cell surface (Supplemental Figure S15c). The findings indicate that CD248, the IR and ITGβ1 form a multi-protein complex on the cell surface.

CD248 dampens insulin binding to the surface of preadipocytes

The close physical interaction of CD248 with the IR and integrin β1, and our findings that insulin sensitivity is heightened by a lack of CD248, raised the possibility that CD248 dampens the functional interaction of insulin with its receptor. To test this hypothesis, we performed binding studies of biotinylated insulin to WT and KO preadipocytes derived from the eWAT of male and female mice (Fig. 8a and b). The rate of specific binding of biotinylated insulin to the surface of equal numbers of preadipocytes was increased with KO cells as compared to WT cells, with saturable equilibrium binding being achieved by 90′ with both WT and KO preadipocytes (not shown). Specific binding of increasing concentrations of biotinylated insulin was measured following a 90′ incubation.[45] For preadipocytes derived from male and female eWAT, the K_D value for KO cells was lower than for WT cells (∼23 nM vs 80 nM for male KO and WT cells, respectively; and ∼40 nM vs 70 nM for female KO and WT cells, respectively) (Fig. 8a and b), consistent with the apparent increased sensitivity of KO cells to insulin.

Soluble CD248 blocks insulin induced phosphorylation of the IR

The IR is the central node for initiating insulin's cellular activities.[46–48] Binding of insulin to extracellular subunits of the IR induces conformational changes in the receptor that are required for its autophosphorylation and subsequent recruitment of adaptor proteins and activation of downstream effectors.[49] We evaluated the effects of soluble CD248 on insulin-induced phosphorylation of purified full-length recombinantly expressed human insulin receptor (IR)[34] in a reaction initiated by the addition of ATP (Supplemental Figure S16a). We first confirmed by Western immunoblotting using a specific antibody, that insulin specifically induces ATP-dependent phosphorylation of the receptor at tyrosines 1162 and 1163 (Supplemental Figure S16b). No suppression of insulin-induced IR phosphorylation was observed when the reaction was allowed to proceed in the presence of the vehicle alone (Fig. 8c), or extracellular fragments of the related lectin-like molecule, thrombomodulin (TMD1).[50] Neither the entire
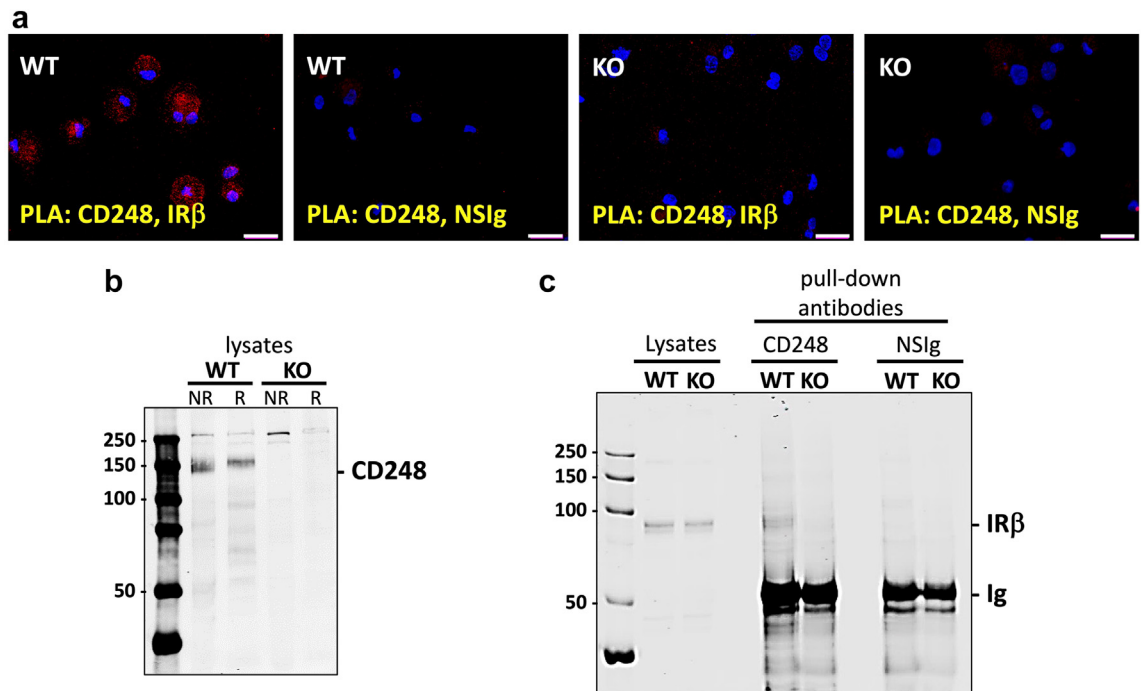
Fig. 7: CD248 and the insulin receptor (IR) are in close proximity to each other. The proximity ligation assay (PLA) was performed on (**a**) purified preadipocytes from WT and KO mice as described in Methods. Species and isotype-matched pre-immune non-specific immunoglobulin (NSIg) were used as controls. Red dots indicate that CD248 and IRβ were in close proximity to each other (size bar = 10 μm). (**b**) Western blot of lysates of preadipocytes WT and KO mice, detected for expression of CD248. (**c**) Pull-downs with anti-CD248 antibodies or NSIg were performed, followed by immunodetection for the IRβ. Anti-CD248 antibodies specifically immunoprecipitated the IR. The blots shown are representative of 3 independent experiments.

extramembranous region of TM (TMD1-3) or the isolated lectin-like domain of TM (TMD1) affected insulin-induced phosphorylation of the IR (Fig. 8c and d; Supplemental Figure S16c). However, pre-incubation of the IR with recombinant soluble CD248 (sCD248)[33] comprising the entire extra-membranous region of the molecule effectively and reproducibly dampened insulin-triggered phosphorylation of the IR (Fig. 8c) in a concentration- and time-dependent manner (Supplemental Figure S16c).

Discussion

In spite of major advances in our understanding of insulin signaling pathways, the mechanisms underlying insulin resistance remain poorly understood. The metabolic consequences of this lack of knowledge are profound, as the numbers of affected individuals with T2D and the associated morbidities and mortality, are steadily rising worldwide.[51] Even the recent and impactful introduction of therapies that reduce insulin requirements[52] are not likely to fully circumvent the need for new approaches that specifically overcome insulin resistance.

In this report, we identify a previously unrecognized mechanism by which the ectodomain of the cell-surface transmembrane glycoprotein, CD248, highly expressed by pre/adipocytes in T2D and obesity,[18] interacts directly with the IR, diminishing its capacity to be autophosphorylated in response to insulin. CD248 thus promotes insulin resistance, i.e., its presence confers resistance to insulin-induced downstream activation/phosphorylation of insulin-dependent pathways, manifest by disorders of glucose uptake and lipid metabolism that are observed in T2D. Reversal of this insulin resistant state could be achieved by reducing CD248 expression, thus conferring protection of mice against diet-induced systemic and adipose tissue glucometabolic and lipid disturbances. Our findings, herein, using a short duration of HFD-induced insulin resistance in male and female mice, insulin clamps, and evidence of relevance in humans, reveal a new direction of research that may yield effective therapeutic approaches to directly overcome insulin resistance.

Insulin is an anabolic hormone that exhibits potent effects on cell growth, glucose homeostasis and lipid metabolism. Its effects are mediated first and foremost via its engagement with the insulin receptor (IR), a
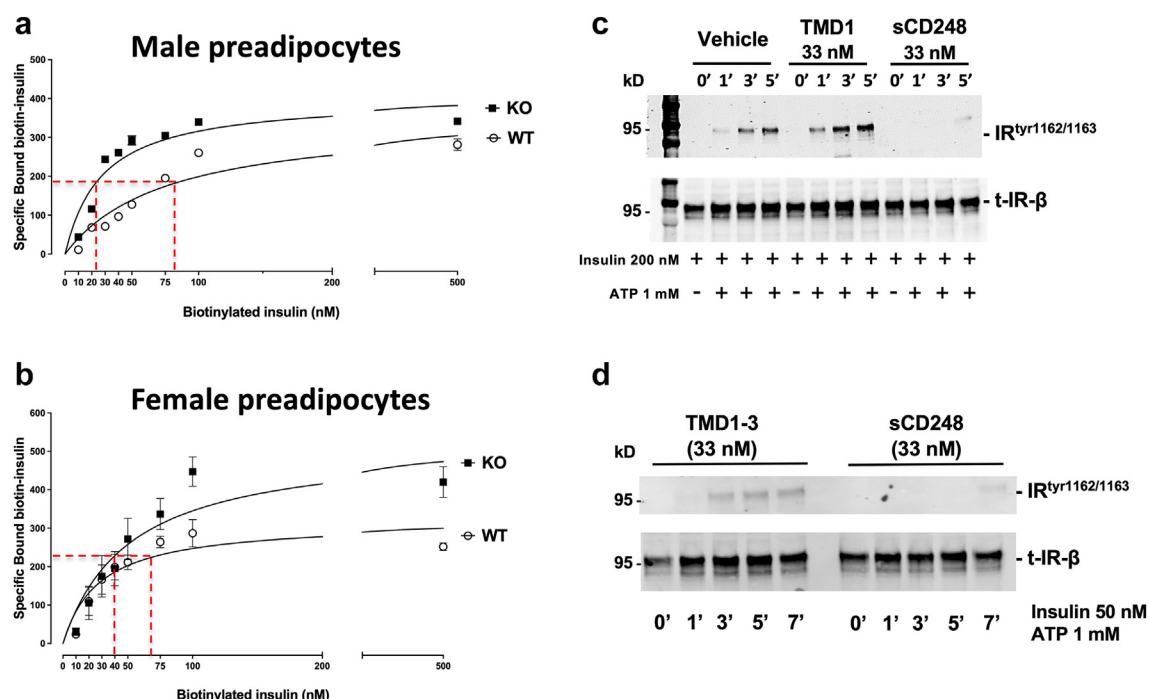
Fig. 8: CD248 reduces insulin binding affinity to its receptor(s) and inhibits insulin-triggered autophosphorylation of the IR. Binding studies were performed using biotinylated insulin on preadipocytes derived from male (**a**) and female mice (**b**). Following experiments to establish the time for equilibrium binding of biotinylated insulin (not shown), cells were incubated with the noted concentrations of biotinylated insulin x 90 min and specific binding (shown) was determined by subtracting the signal obtained with 10 μM nonbiotinylated insulin and binding affinities (K_D) were calculated. (**c–d**) Purified recombinant human IR was incubated with 33 nM sCD248, 33 nM thrombomodulin (TMD1-3), 33 nM TMD1 or vehicle alone in the presence of 200 nM insulin (c) or 50 nM insulin (d) for varying periods of time in the presence or absence of 1 mM ATP. An additional vehicle alone control for D is in Supplemental Figure S16c. Reactants were separated for Western immunoblotting to detect insulin-induced autophosphorylation of the IR with specific antibodies.

member of a family of growth factors with tyrosine kinase activity.[53–55] The IR exists as a heterotetramer, comprising pairs of extracellular and membrane/cytoplasmic subunits that contain tyrosine kinase domains.[46–49] Structural studies reveal that insulin binds sequentially to the IR via two distinct extracellular regions,[53] whereupon the receptor undergoes large conformational changes that allow it to be autophosphorylated at several tyrosine residues. This in turn leads to activation of the IR kinase and subsequent tyrosine phosphorylation of insulin receptor substrate (IRS) proteins.[56] The IR and IRS proteins are key nodes for a network of interactions with several other intracellular proteins that mediate downstream signaling events that modulate cell growth, differentiation, lipid metabolism and glucometabolism. Differential interactions of these intracellular proteins with the IR and IRS proteins are critical in regulating specificity and sensitivity of signaling in response to insulin, tightly controlled to maintain homeostasis under a range of stresses. Disruptions in their integrity may result in diminished sensitivity to insulin, with consequential defects in cell growth and differentiation, glucose homeostasis and lipid metabolism.[57]

Molecular mechanisms underlying insulin resistance have primarily been attributed to alterations in insulin signaling downstream of the IR, impacting on one or both of the canonical pathways, often with effects on IR trafficking/internalization that may affect IR expression levels.[58,59] Of the >100 naturally occurring mutations and splicing abnormalities of the IR that have been reported,[60] the majority are associated with extreme insulin resistance, and not representative of insulin resistance typically seen with T2D and obesity. However, more relevant to the vast majority of T2D cases, multiple binding partners for the IR have been identified, including for example, protein tyrosine phosphatase (PTP)-1B, ninjurin-2, suppressor of cytokine signaling (SOCS) proteins and Grb proteins.[57,61–66] These are located in the cell or cell membrane, where they variably modulate IR activity and insulin sensitivity. Although the rare type B syndrome of insulin resistance is caused by anti-IR antibodies that block insulin binding,[67] few naturally occurring proteins that impact on insulin sensitivity have been described that bind to the extracellular subunits of the IR. Such protein-IR interactions might, however, be more amenable to therapeutic targeting.

CD248 is a type I transmembrane glycoprotein that comprises an N-terminal lectin-like domain, a sushi domain, 3 EGF-like repeats, a mucin-like region, a transmembrane domain and a cytoplasmic tail.[16,68,69] The lectin-like domain binds to extracellular matrix proteins[70,71] and modulates macrophage activation in mouse models of sepsis.[33] The cytoplasmic tail contains sites for potential phosphorylation and a C-terminal PDZ-binding motif[72] that may regulate cell signaling.[16,20] In this report, we showed that preadipocytes that express CD248 are less sensitive to insulin stimulation than those lacking CD248, with reduced phosphorylation of MAP kinase Erk1/2 and AKT, and in turn, lower expression of phosphorylated GSK3β. Similar CD248-dependent differences in insulin-triggered AKT phosphorylation were observed with primary cultured adipocytes derived from visceral adipose tissue from a small cohort of individuals with obesity. This CD248-dependent differential response was not due to altered expression of the IR, as levels of the IR were unaffected by deletion of *CD248* or by exposure to insulin during the experiments. Our insulin binding studies indicated that CD248 on the preadipocyte cell surface, dampens the affinity to its cognate cell surface receptor(s). We did not exclude the possibility that CD248 triggers internalization of the IR. We did not uncover a specific interaction of CD248 with insulin (data not shown), but did confirm, using pull-downs and proximity ligation assays, that integral membrane CD248 interacts directly with the IR expressed on the surface of preadipocytes.

These findings led us to test whether CD248, in a purified system, could regulate insulin-triggered autophosphorylation of the IR. To that end, we used recombinant full-length human IR that was purified in a detergent solubilized form, such that it retains its autophosphorylation and kinase activity.[34] We reacted the IR with insulin and ATP and varying concentrations of soluble CD248 representing the entire ectodomain. By measuring IR autophosphorylation, we showed that this soluble form of CD248 effectively suppressed IR autophosphorylation. Studies are ongoing to delineate which structure(s) of CD248 functionally interacts with the IR to abrogate insulin binding and insulin-induced autophosphorylation of the IR, and where these bind to the IR. We are also testing whether CD248 triggers IR internalization, an additional potential mechanism of regulating insulin signaling.[58] The information gained will be important for the design of interventions that abrogate CD248 binding to the IR to overcome insulin resistance.

The paradigm of CD248 acting as a sensor that modulates the function of a cell surface-expressed protein by inducing allosteric changes affecting its relationship to its ligand, is not entirely new. We recently showed that on the surface of vascular smooth muscle cells and monocytes, CD248 participates in assembly of the integral membrane protein tissue factor (TF), with factor VIIa and factor X, forming a multi-molecular complex that is critical for initiation of the clotting cascade.[22] There, CD248 acts as a scaffold for factor X, triggering allosteric changes and the spatial re-alignment of factor X with the TF-factor VIIa complex, thereby enhancing coagulation activation. In models of arterial and venous thrombosis, mice lacking CD248, thus are relatively protected against stress-induced clot formation, as compared to WT counterparts.[22] It is worth noting that, like CD248, the prothrombotic/proinflammatory TF is also expressed by pre/adipocytes[73]; and it is well known that obesity and insulin resistance are associated with a heightened risk of atherothrombosis. Studies to delineate potential cross-talk between the coagulation related TF-factor VIIa-factor X complex and the insulin-IR signaling system in the context of CD248, are ongoing.

In comparing WT and KO mice, we established that even after a 2 week HFD, lack of CD248 rendered male mice resistant to systemic disturbances in glucose metabolism and insulin sensitivity, as measured by the GTT and ITT. These CD248-dependent effects on glucose metabolism were also confirmed in the gold-standard insulin clamp studies. After this relatively short exposure time to the HFD, plasma levels of triglycerides were unaffected, and hepatic accumulation of triglycerides was only slightly increased over that seen with WT mice. However, significant localized improvements in glucose uptake and lipolysis were readily evident in all WAT depots examined, albeit with some variability. The protective effects of deletion of CD248 on glucose homeostasis and lipid metabolism in the WAT occurred in parallel with significantly heightened WAT levels of GLUT4, increased phosphorylation of AKT, GSK3β, and p70S6, and reduced levels of ATGL, all in line with augmented insulin sensitivity, with greater glucose uptake and dampened lipolysis. We did not detect CD248-dependent baseline differences in GTT or ITT in the mice before or after a 2 week NCD. However, we did observe increased glucose uptake in eWAT explants and corresponding increases in GLUT4 and phosphorylated AKT and GSK3β in iWAT and eWAT from NCD-fed KO mice. Although the insulin clamps studies did not reveal CD248-dependent changes in glucose kinetics in NCD-fed mice, the explant studies suggest that WAT of KO mice may be more sensitive to insulin even following a NCD, prior to the emergence of other manifestations of T2D. Indeed, glucose uptake was also increased in WAT explants in the absence of exogenous insulin. While the mechanisms remain a mystery, this might be related to non-insulin mediated GLUT4 translocation to the membrane of KO adipocytes, and/or to the action of other glucose transporters that are less reliant on insulin, such as GLUT1.[41] Our findings also raise the intriguing possibility that CD248 acts as an insulin desensitizer in normal conditions to limit overactivation

of insulin signaling. Insulin resistance develops in prolonged fasting, and not only under obese conditions.[74] It is thus reasonable to consider that subtle changes in expression or orientation of CD248 relative to insulin and the IR, may fine-tune insulin signaling in response to glucometabolic changes that normally occur in healthy individuals. Further study is required to clarify these observations and test these hypotheses.

It is notable that all of our studies–*in vivo* and *ex vivo*–showed that lack of CD248 improved glucose metabolism by enhancing insulin sensitivity in WAT, but not in skeletal muscle. The insulin clamp studies further demonstrated that CD248 deficiency resulted in enhanced sensitivity of the liver to suppress glucose production. These findings are also consistent with our previous work, in which adipocyte-specific KO mice exhibited heightened sensitivity to insulin, and the mice were thus protected against HFD-induced glucometabolic disturbances.[18] Others have identified targeted defects in insulin action in adipocytes that result in systemic insulin resistance with alterations in esterification of fatty acids, lipid biosynthesis and impaired adipogenesis.[75] Although adipose tissue only takes up ~10% of the glucose load after a meal, the evidence strongly supports its central role in regulating whole body insulin sensitivity.[4]

Using different lines of genetically modified WT and KO mice, the groups of Naylor and colleagues recently reported results of similar studies, stressing the mice however, with a 13 week HFD.[26,76] They also found that deletion of CD248 provided protection against HFD-induced obesity and glucometabolic disturbances, with depot-specific changes in fat accumulation; but the differences were strikingly less than what we observed. Indeed, throughout the time course of the HFD in their studies, they did not detect any changes in glucose uptake based on GTT. They did not examine insulin signaling pathways in the WAT or isolated pre/adipocytes. Moreover, in their studies, female KO mice as compared to their WT counterparts were entirely unaffected by loss of CD248, leading them to conclude that CD248 has a sex-specific (male) role in lipid deposition in mice. Our findings would argue against that premise, and we would rather conclude that glucometabolism in female mice is sensitive to deletion of CD248 but to a lesser extent than males; and thus, that CD248 plays a role in glucose homeostasis and lipid metabolism in both sexes in mice. As Naylor and colleagues pointed out,[26,76] the reasons behind the variances in responses in their studies and ours, may be due to differences in mouse strain, housing and other unidentified factors. We did not evaluate the mechanisms underlying sex-dependent differences in glucometabolic function observed in our mice. However, such differences have long been recognized, and many groups are actively attempting to gain new insights (reviewed[77,78]). Estrogens regulate metabolic processes related to energy balance, impact inflammatory responses and modulate expression of genes that regulate glycolipid metabolism in fat tissue.[79] Studies in humans confirm that there are sex-dependent differences in insulin secretion and sensitivity, and that females oxidize more lipids and less carbohydrates, produce less hepatic glucose, and deplete less glycogen from muscle.[77,80,81] Multiple studies in mice have reported variable tissue-specific effects of sex hormones on insulin sensitivity and insulin signaling pathway activities.[78,82,83] Most conclude that females exhibit higher insulin sensitivity and lower muscle mass that favours greater WAT energy storage capacity. In spite of much work, the mechanisms that underly sex-dependent differences in insulin sensitivity remain incompletely understood. We have not noted sex-dependent differences in CD248 expression in the mice, and thus the potential participation of CD248 in the sex-dependent differences is unknown. These knowledge gaps are strong rationale for incorporating sex in all such studies.[84,85]

Our finding that soluble CD248 can regulate insulin signaling at the level of the IR, may be of *in vivo* pathophysiologic relevance. Soluble forms of CD248 are known to circulate in the blood, these being generated during inflammatory and proliferative states by shedding from the cell surface, whereupon they may exhibit autocrine and paracrine activities.[86] A soluble form of CD248 that is likely the entire ectodomain (based on the reported molecular weight) can be released by mesenchymal stem cells, shed in parallel with pro-angiogenic factors in an MMP-dependent manner from the cell surface by IL-1β.[87] In the context of our findings, it is particularly intriguing that in early pregnancy, maternal plasma levels of CD248 were higher in a group of women with gestational diabetes as compared to a control group of pregnant women.[88] We hypothesize that the increase in soluble CD248 in gestational diabetes, might not only be an association, but rather it might contribute to the insulin resistance by blocking insulin signaling via the IR.

Recently, Lu et al.[89] reported that CD248 promotes integrin β1 interactions with extracellular matrix proteins that in turn induce changes in cell–cell interactions. Integrin β1-extracellular matrix interactions modulate glucose homeostasis and insulin sensitivity as adipose tissue undergoes remodeling in response to dietary changes.[44,90] This may occur at least in part, via activation of the focal adhesion kinase (FAK)-paxillin pathway, elevations of which have been associated with enhanced insulin resistance in mice and humans.[91] Interestingly, integrin β1 also binds directly to extracellular subunits of the IR[44] whereupon it may facilitate insulin signaling. We show that in addition to binding to the IR, CD248 also interacts directly with integrin β1. Moreover, via its lectin-like domain, CD248 binds to several other extracellular matrix proteins, including fibronectin, collagen types I

and IV, and multimerin 2.[70,71] The complexities and relevance of the trimolecular assembly of CD248, the IR and integrin β1 in the context of an extracellular matrix that undergoes diet induced remodeling, remain to be elucidated.

Interestingly, activation of FAK that occurs in response to a HFD[91] is also correlated with tumour growth[92] and thus, CD248 and integrin-β1 might co-operate to promote tumorigenesis via effects on FAK activation. Indeed, CD248 is markedly upregulated in multiple cells of mesenchymal origin (e.g., perivascular smooth muscle cells, pericytes, stromal fibroblasts, osteoblasts) during tumour growth, the extent of which may be correlated with prognosis.[21,93,94] There is strong evidence to support a role for CD248 in facilitating tumour growth via multiple mechanisms that include, for example, vascular remodeling that is associated with activation of hypoxia inducible factors, release of angiogenic factors, recruitment of inflammatory leukocytes and upregulation of pro-fibrotic genes.[15–17] Several groups have shown that deletion of CD248 in mice is largely without adverse effects, and furthermore confers protection from the growth of several tumors.[20] This has triggered considerable interest in therapeutically targeting CD248 for various cancers.[95] That obesity and insulin resistance are also associated with a heightened risk of cancer,[96] implies a yet-to-be clarified molecular link between those tumours associated with T2D and CD248.

Diabetic kidney disease is a common complication of T2D, the risk of which correlates with the severity of insulin resistance.[97] Insulin-triggered cross-talk between renal mesangial cells and podocytes dampens endoplasmic reticulum (ER)-associated degradative pathways that otherwise promote renal glomerular cell damage and kidney dysfunction that is a feature of diabetic kidney disease.[98] Krishnan et al.[99] recently found that glucose-stressed mesangial cells responded with markedly increased expression of CD248 which in turn, triggered a renal glomerular-damaging maladaptive unfolded protein response (UPR) by inhibiting cytoprotective splicing of an ER transcription factor, X-box binding protein-1 (XBP1). This glucose-induced UPR response was ameliorated in mesangial cells that lack CD248. Interestingly, at least in podocytes, it is believed that the UPR response is normally held in check by insulin signaling via the IR which non-canonically activates the protective spliced XBP1.[100] In mouse models of diabetes, impaired insulin signaling thus propagates a hyperglycemia-induced maladaptive UPR which results in diabetic nephropathy. While podocytes are not known to express CD248, intraglomerular cross-talk between these cells occurs in the regulation of ER-associated degradation in diabetic kidney disease.[98] We hypothesize that in the setting of chronic hyperglycemia, the augmented expression of CD248 by mesangial cells, interferes with insulin-triggered autophosphorylation of

the IR expressed by podocytes and the mesangial cells, blocking splicing of the protective SBP1. Thus, abrogating the CD248-IR interaction may yield a means of dampening the progression of diabetic nephropathy.

In patients with severe sepsis, even in the absence of underlying diabetes or obesity, hyperglycemia frequently occurs, contributing to widespread organ dysfunction and increased risk of death.[101–103] The pathophysiology of the hyperglycemia is complex, but minimally involves elevations in catecholamines, cytokines, growth factors, and cortisol that lead to excessive hepatic glucose production and peripheral insulin resistance.[102,104] While TNFα and IL-6 have been implicated in sepsis-associated insulin resistance, we were unable to discern any effect of these cytokines on CD248 expression in cultured mesenchymal cells.[105] On the other hand, CD248 could contribute to the insulin resistance, as it is upregulated by hypoxia[15] and glucose,[99] both of which are prominent features of this condition. Overall, the serious nature of the glucometabolic disorder in these patients warrants further study, and the potential role of CD248 should be considered.

Numerous strategies are being pursued toward the development of safe and specific pharmacologic approaches to overcome insulin resistance. This includes targeting one or more of the many intracellular signaling pathways and regulators of phosphorylation that are implicated in controlling insulin sensitivity. Several of these attempts have shown efficacy in preclinical trials, but have not yet entered into or met with similar success in human studies. These include, for example, NF-κB, SOCS proteins, components of the JNK and Wnt signaling pathways and the protein tyrosine phosphatase (PTP)-1B (reviewed[65,106,107]). By their very location inside the cell, these are challenging targets to access pharmacologically.

Our identification of a potential mechanism of enhancing insulin sensitivity on the cell surface by blocking binding of CD248 to the IR, provides a previously unrecognized and likely a more accessible approach to overcome the insulin resistant state. Such a strategy would not come without challenges. While a systemic therapy may efficiently bathe the highly vascular adipose tissue, specifically targeting WAT pre/adipocytes with, for example, drugs, antibodies, compounds or siRNAs, without affecting other tissues/organs to avoid off-target effects, is not yet feasible. However, there are ample data that support the safety of dampening expression and/or the function of CD248 for therapeutic purposes. CD248 knockout mice are healthy and fertile, without evidence of increased susceptibility to disease. They are protected against inflammation and fibrosis of several organ systems,[16,24,99,108] from atherosclerosis,[21] tumor growth,[20] thrombosis,[22] sepsis[33] and diet induced obesity,[18] and also do not exhibit adverse effects on wound healing/repair.[19] Indeed, in recent extensive studies in mice,

administration of anti-CD248 antibodies "caused no obvious toxicity in ... brain, heart, liver, lung, kidney and spleen." When administered during pregnancy, the antibodies also did not cause any embryonic developmental defects in the murine offspring.[109] Finally, anti-CD248 antibodies have been safely administered to humans in several clinical trials, albeit some to patients with cancer where it might be difficult to assess for side effects.[110,111] Nonetheless, the evidence for CD248 being a safe target is strong (reviewed in,[95,109,112,113]) and its cell-surface functional expression, makes it an attractive one to explore to overcome insulin resistance.

Finally, we have not excluded the possibility that CD248 may promote insulin resistance and adipose tissue dysfunction by additional mechanisms beyond its binding and blocking the function of the IR and/or triggering the receptor's internalization. This may include, for example, altering the extracellular matrix in metabolically active tissues, promoting inflammation, and/or dysregulating angiogenesis and fibrosis. We also do not understand how/why CD248 is increased in some individuals and not in others, and what epi/genetic and/or environmental factors cause it to increase in various states. Our findings that adipose/adipocyte CD248 transcript levels rise in response to a HFD and in obesity and return toward normal in humans following bariatric surgery,[18] suggest that changes in adipose tissue structure/function trigger the increase in CD248. However, without dietary or pharmacologic intervention, this is likely to initiate a positive feedback loop, as increased CD248 further promotes adipose tissue hypoxia, dysfunction and worsening insulin resistance.

Overall, we have uncovered a previously unrecognized mechanism by which the extracellular region of CD248 promotes insulin resistance by directly binding to the IR. This molecular interaction constitutes a safe and potentially uniquely accessible therapeutic target to prevent/reverse insulin resistance.

References
1 Rose DP, Gracheck PJ, Vona-Davis L. The interactions of obesity, inflammation and insulin resistance in breast cancer. *Cancers.* 2015;7(4):2147–2168.
2 Lakka HM, Laaksonen DE, Lakka TA, et al. The metabolic syndrome and total and cardiovascular disease mortality in middle-aged men. *JAMA.* 2002;288(21):2709–2716.
3 Borch KH, Nyegaard C, Hansen JB, et al. Joint effects of obesity and body height on the risk of venous thromboembolism: the Tromso Study. *Arterioscler Thromb Vasc Biol.* 2011;31(6):1439–1444.
4 Santoro A, Kahn BB. Adipocyte regulation of insulin sensitivity and the risk of type 2 diabetes. *N Engl J Med.* 2023;388(22):2071–2085.
5 Rabiee A, Kruger M, Ardenkjaer-Larsen J, Kahn CR, Emanuelli B. Distinct signalling properties of insulin receptor substrate (IRS)-1 and IRS-2 in mediating insulin/IGF-1 action. *Cell Signal.* 2018;47:1–15.
6 Boucher J, Kleinridders A, Kahn CR. Insulin receptor signaling in normal and insulin-resistant states. *Cold Spring Harbor Perspect Biol.* 2014;6(1).
7 Taniguchi CM, Emanuelli B, Kahn CR. Critical nodes in signalling pathways: insights into insulin action. *Nat Rev.* 2006;7(2):85–96.
8 Chiefari E, Mirabelli M, La Vignera S, et al. Insulin resistance and cancer: in search for a causal link. *Int J Mol Sci.* 2021;22(20).
9 Fazakerley DJ, Krycer JR, Kearney AL, Hocking SL, James DE. Muscle and adipose tissue insulin resistance: malady without mechanism? *J Lipid Res.* 2019;60(10):1720–1732.
10 Lin D, Chun TH, Kang L. Adipose extracellular matrix remodelling in obesity and insulin resistance. *Biochem Pharmacol.* 2016;119:8–16.
11 Crewe C, An YA, Scherer PE. The ominous triad of adipose tissue dysfunction: inflammation, fibrosis, and impaired angiogenesis. *J Clin Invest.* 2017;127(1):74–82.
12 Arcidiacono B, Chiefari E, Foryst-Ludwig A, et al. Obesity-related hypoxia via miR-128 decreases insulin-receptor expression in human and mouse adipose tissue promoting systemic insulin resistance. *eBioMedicine.* 2020;59:102912.
13 Regazzetti C, Peraldi P, Gremeaux T, et al. Hypoxia decreases insulin signaling pathways in adipocytes. *Diabetes.* 2009;58(1):95–103.
14 Trayhurn P, Wang B, Wood IS. Hypoxia in adipose tissue: a basis for the dysregulation of tissue function in obesity? *Br J Nutr.* 2008;100(2):227–235.
15 Ohradanova A, Gradin K, Barathova M, et al. Hypoxia upregulates expression of human endosialin gene via hypoxia-inducible factor 2. *Br J Cancer.* 2008;99(8):1348–1356.
16 Maia M, de Vriese A, Janssens T, et al. CD248 and its cytoplasmic domain: a therapeutic target for arthritis. *Arthritis Rheum.* 2010;62(12):3595–3606.
17 Brett E, Zielins ER, Chin M, et al. Isolation of CD248-expressing stromal vascular fraction for targeted improvement of wound healing. *Wound Repair Regen.* 2017;(3):414–422.
18 Petrus P, Fernandez TL, Kwon MM, et al. Specific loss of adipocyte CD248 improves metabolic health via reduced white adipose tissue hypoxia, fibrosis and inflammation. *EBioMedicine.* 2019;44:489–501.
19 Nanda A, Karim B, Peng Z, et al. Tumor endothelial marker 1 (Tem1) functions in the growth and progression of abdominal tumors. *Proc Natl Acad Sci U S A.* 2006;103(9):3351–3356.
20 Maia M, DeVriese A, Janssens T, et al. CD248 facilitates tumor growth via its cytoplasmic domain. *BMC Cancer.* 2011;11:162.

21 Hasanov Z, Ruckdeschel T, Konig C, et al. Endosialin promotes atherosclerosis through phenotypic remodeling of vascular smooth muscle cells. *Arterioscler Thromb Vasc Biol.* 2017;37(3):495–505.

22 Kapopara PR, Safikhan NS, Huang JL, et al. CD248 enhances tissue factor (TF) procoagulant function, promoting arterial and venous thrombosis in mouse models. *J Thromb Haemost.* 2021;19(8):1932–1947.

23 Mogler C, Wieland M, Konig C, et al. Hepatic stellate cell-expressed endosialin balances fibrogenesis and hepatocyte proliferation during liver damage. *EMBO Mol Med.* 2015;7(3):332–338.

24 Smith SW, Croft AP, Morris HL, et al. Genetic deletion of the stromal cell marker CD248 (endosialin) protects against the development of renal fibrosis. *Nephron.* 2015;131(4):265–277.

25 Pai CH, Lin SR, Liu CH, et al. Targeting fibroblast CD248 attenuates CCL17-expressing macrophages and tissue fibrosis. *Sci Rep.* 2020;10(1):16772.

26 Patrick K, Tian X, Cartwright D, et al. Sex-specific effects of CD248 on metabolism and the adipose tissue lipidome. *PLoS One.* 2023;18(4):e0284012.

27 Hausman DB, Park HJ, Hausman GJ. Isolation and culture of preadipocytes from rodent white adipose tissue. *Methods Mol Biol.* 2008;456:201–219.

28 Jain K, Verma PJ, Liu J. Isolation and handling of mouse embryonic fibroblasts. *Methods Mol Biol.* 2014;1194:247–252.

29 Pereira MJ, Palming J, Rizell M, et al. The immunosuppressive agents rapamycin, cyclosporin A and tacrolimus increase lipolysis, inhibit lipid storage and alter expression of genes involved in lipid metabolism in human adipose tissue. *Mol Cell Endocrinol.* 2013;365(2):260–269.

30 Pereira MJ, Palming J, Rizell M, et al. mTOR inhibition with rapamycin causes impaired insulin signalling and glucose uptake in human subcutaneous and omental adipocytes. *Mol Cell Endocrinol.* 2012;355(1):96–105.

31 Yamamoto N, Ueda-Wakagi M, Sato T, et al. Measurement of glucose uptake in cultured cells. *Curr Protoc Pharmacol.* 2015;71:12 4 1–124 26.

32 Shi CS, Shi GY, Hsiao SM, et al. Lectin-like domain of thrombomodulin binds to its specific ligand Lewis Y antigen and neutralizes lipopolysaccharide-induced inflammatory response. *Blood.* 2008;112(9):3661–3670.

33 Cheng TL, Lin YS, Hong YK, et al. Role of tumor endothelial marker 1 (Endosialin/CD248) lectin-like domain in lipopolysaccharide-induced macrophage activation and sepsis in mice. *Transl Res.* 2021;232:150–162.

34 Delle Bovi RJ, Miller WT. Expression and purification of functional insulin and insulin-like growth factor 1 holoreceptors from mammalian cells. *Anal Biochem.* 2017;536:69–77.

35 Jarmoskaite I, AlSadhan I, Vaidyanathan PP, Herschlag D. How to measure and evaluate binding affinities. *Elife.* 2020;9:e57264. https://doi.org/10.7554/eLife.57264.

36 Ayala JE, Bracy DP, McGuinness OP, Wasserman DH. Considerations in the design of hyperinsulinemic-euglycemic clamps in the conscious mouse. *Diabetes.* 2006;55(2):390–397.

37 Alquier T, Poitout V. Considerations and guidelines for mouse metabolic phenotyping in diabetes research. *Diabetologia.* 2018;61(3):526–538.

38 Yue JT, Abraham MA, Bauer PV, et al. Inhibition of glycine transporter-1 in the dorsal vagal complex improves metabolic homeostasis in diabetes and obesity. *Nat Commun.* 2016;7:13501.

39 Cignarelli A, Genchi VA, Perrini S, Natalicchio A, Laviola L, Giorgino F. Insulin and insulin receptors in adipose tissue development. *Int J Mol Sci.* 2019;20(3):759.

40 Wang L, Li J, Di LJ. Glycogen synthesis and beyond, a comprehensive review of GSK3 as a key regulator of metabolic pathways and a therapeutic target for treating metabolic diseases. *Med Res Rev.* 2022;42(2):946–982.

41 Chadt A, Al-Hasani H. Glucose transporters in adipose tissue, liver, and skeletal muscle in metabolic health and disease. *Pflugers Arch.* 2020;472(9):1273–1298.

42 Miyoshi H, Perfield JW 2nd, Obin MS, Greenberg AS. Adipose triglyceride lipase regulates basal lipolysis and lipid droplet size in adipocytes. *J Cell Biochem.* 2008;105(6):1430–1436.

43 Arkun Y. Dynamic modeling and analysis of the cross-talk between insulin/AKT and MAPK/ERK signaling pathways. *PLoS One.* 2016;11(3):e0149684.

44 Ruiz-Ojeda FJ, Wang J, Backer T, et al. Active integrins regulate white adipose tissue insulin sensitivity and brown fat thermogenesis. *Mol Metabol.* 2021;45:101147.

45 Torlinska T, Mackowiak P, Nogowski L, Nowak KW, Madry E, Perz M. Characteristics of insulin receptor binding to various rat tissues. *J Physiol Pharmacol.* 1998;49(2):261–270.

46 Gutmann T, Kim KH, Grzybek M, Walz T, Coskun U. Visualization of ligand-induced transmembrane signaling in the full-length human insulin receptor. *J Cell Biol.* 2018;217(5):1643–1649.

47 Park J, Li J, Mayer JP, et al. Activation of the insulin receptor by an insulin mimetic peptide. *Nat Commun.* 2022;13(1):5594.

48 Nielsen J, Brandt J, Boesen T, et al. Structural investigations of full-length insulin receptor dynamics and signalling. *J Mol Biol.* 2022;434(5):167458.

49 Lawrence MC. Understanding insulin and its receptor from their three-dimensional structures. *Mol Metabol.* 2021;52:101255.

50 Valdez Y, Maia M, Conway EM. CD248: reviewing its role in health and disease. *Curr Drug Targets.* 2012;13(3):432–439.

51 Chew NWS, Ng CH, Tan DJH, et al. The global burden of metabolic disease: data from 2000 to 2019. *Cell Metabol.* 2023;35(3):414–428 e3.

52 Drucker DJ. Mechanisms of action and therapeutic application of glucagon-like peptide-1. *Cell Metabol.* 2018;27(4):740–756.

53 Choi E, Bai XC. The activation mechanism of the insulin receptor: a structural perspective. *Annu Rev Biochem.* 2023;92:247–272.

54 Weiss MA, Lawrence MC. A thing of beauty: structure and function of insulin's "aromatic triplet". *Diabetes Obes Metab.* 2018;20 Suppl 2(Suppl 2):51–63.

55 Saltiel AR. Insulin signaling in health and disease. *J Clin Invest.* 2021;131(1).

56 Hanke S, Mann M. The phosphotyrosine interactome of the insulin receptor family and its substrates IRS-1 and IRS-2. *Mol Cell Proteomics.* 2009;8(3):519–534.

57 Pei J, Wang B, Wang D. Current studies on molecular mechanisms of insulin resistance. *J Diabetes Res.* 2022;2022:1863429.

58 Carpentier JL. Insulin receptor internalization: molecular mechanisms and physiopathological implications. *Diabetologia.* 1994;37(Suppl 2):S117–S124.

59 Lee SH, Park SY, Choi CS. Insulin resistance: from mechanisms to therapeutic strategies. *Diabetes Metab J.* 2022;46(1):15–37.

60 Rojek A, Niedziela M. [Insulin receptor defect as a cause of Rabson-Mendenhall syndrome and other rare genetic insulin resistance syndromes]. *Pediatr Endocrinol Diabetes Metab.* 2010;16(3):205–212.

61 Virkamaki A, Ueki K, Kahn CR. Protein-protein interaction in insulin signaling and the molecular mechanisms of insulin resistance. *J Clin Invest.* 1999;103(7):931–943.

62 Xue B, Kim YB, Lee A, et al. Protein-tyrosine phosphatase 1B deficiency reduces insulin resistance and the diabetic phenotype in mice with polygenic insulin resistance. *J Biol Chem.* 2007;282(33):23829–23840.

63 Peng H, Yu Y, Wang P, et al. NINJ2 deficiency inhibits pre-adipocyte differentiation and promotes insulin resistance through regulating insulin signaling. *Obesity.* 2023;31(1):123–138.

64 Ding X, Iyer R, Novotny C, et al. Inhibition of Grb14, a negative modulator of insulin signaling, improves glucose homeostasis without causing cardiac dysfunction. *Sci Rep.* 2020;10(1):3417.

65 Suren Garg S, Kushwaha K, Dubey R, Gupta J. Association between obesity, inflammation and insulin resistance: insights into signaling pathways and therapeutic interventions. *Diabetes Res Clin Pract.* 2023;200:110691.

66 Youn DY, Xiaoli AM, Kwon H, Yang F, Pessin JE. The subunit assembly state of the Mediator complex is nutrient-regulated and is dysregulated in a genetic model of insulin resistance and obesity. *J Biol Chem.* 2019;294(23):9076–9083.

67 Kahn CR, Flier JS, Bar RS, et al. The syndromes of insulin resistance and acanthosis nigricans. Insulin-receptor disorders in man. *N Engl J Med.* 1976;294(14):739–745.

68 Opavsky R, Haviernik P, Jurkovicova D, et al. Molecular characterization of the mouse tem1/endosialin gene regulated by cell density in vitro and expressed in normal tissues in vivo. *J Biol Chem.* 2001;276(42):38795–38807.

69 Rettig WJ, Garin-Chesa P, Healey JH, Su SL, Jaffe EA, Old LJ. Identification of endosialin, a cell surface glycoprotein of vascular endothelial cells in human cancer. *Proc Natl Acad Sci U S A.* 1992;89(22):10832–10836.

70 Khan KA, Naylor AJ, Khan A, et al. Multimerin-2 is a ligand for group 14 family C-type lectins CLEC14A, CD93 and CD248 spanning the endothelial pericyte interface. *Oncogene.* 2017;36(44):6097–6108.

71 Tomkowicz B, Rybinski K, Foley B, et al. Interaction of endosialin/TEM1 with extracellular matrix proteins mediates cell adhesion and migration. *Proc Natl Acad Sci U S A*. 2007;104(46):17965–17970.

72 Greenlee MC, Sullivan SA, Bohlson SS. CD93 and related family members: their role in innate immunity. *Curr Drug Targets*. 2008;9(2):130–138.

73 Eden D, Panagiotou G, Mokhtari D, Eriksson JW, Aberg M, Siegbahn A. Adipocytes express tissue factor and FVII and are procoagulant in a TF/FVIIa-dependent manner. *Ups J Med Sci*. 2019;124(3):158–167.

74 Shin J, Fukuhara A, Onodera T, et al. SDF-1 is an autocrine insulin-desensitizing factor in adipocytes. *Diabetes*. 2018;67(6):1068–1078.

75 Yore MM, Syed I, Moraes-Vieira PM, et al. Discovery of a class of endogenous mammalian lipids with anti-diabetic and anti-inflammatory effects. *Cell*. 2014;159(2):318–332.

76 Armitage EG, Barnes A, Patrick K, et al. Metabolic consequences for mice lacking Endosialin: LC-MS/MS-based metabolic phenotyping of serum from C56Bl/6J Control and CD248 knock-out mice. *Metabolomics*. 2021;17(2):14.

77 Varlamov O, Bethea CL, Roberts CT Jr. Sex-specific differences in lipid and glucose metabolism. *Front Endocrinol*. 2014;5:241.

78 Tramunt B, Smati S, Grandgeorge N, et al. Sex differences in metabolic regulation and diabetes susceptibility. *Diabetologia*. 2020;63(3):453–461.

79 De Paoli M, Zakharia A, Werstuck GH. The role of estrogen in insulin resistance: a review of clinical and preclinical data. *Am J Pathol*. 2021;191(9):1490–1498.

80 Broussard JL, Perreault L, Macias E, et al. Sex differences in insulin sensitivity are related to muscle tissue acylcarnitine but not subcellular lipid distribution. *Obesity*. 2021;29(3):550–561.

81 Basu R, Dalla Man C, Campioni M, et al. Effects of age and sex on postprandial glucose metabolism: differences in glucose turnover, insulin secretion, insulin action, and hepatic insulin extraction. *Diabetes*. 2006;55(7):2001–2014.

82 Macotela Y, Boucher J, Tran TT, Kahn CR. Sex and depot differences in adipocyte insulin sensitivity and glucose metabolism. *Diabetes*. 2009;58(4):803–812.

83 Gao A, Su J, Liu R, et al. Sexual dimorphism in glucose metabolism is shaped by androgen-driven gut microbiome. *Nat Commun*. 2021;12(1):7080.

84 Ingvorsen C, Karp NA, Lelliott CJ. The role of sex and body weight on the metabolic effects of high-fat diet in C57BL/6N mice. *Nutr Diabetes*. 2017;7(4):e261.

85 Tiraby C, Tavernier G, Capel F, et al. Resistance to high-fat-diet-induced obesity and sexual dimorphism in the metabolic responses of transgenic mice with moderate uncoupling protein 3 overexpression in glycolytic skeletal muscles. *Diabetologia*. 2007;50(10):2190–2199.

86 Feng WH, Chen PS, Chung HC, Lin YH, Li YH. Soluble tumor endothelial marker 1 in heart failure with reduced ejection fraction: a pilot study. *Front Cardiovasc Med*. 2022;9:1015471.

87 Payet M, Ah-Pine F, Guillot X, Gasque P. Inflammatory mesenchymal stem cells express abundant membrane-bound and soluble forms of C-type lectin-like CD248. *Int J Mol Sci*. 2023;24(11).

88 Wei Y, He A, Huang Z, Liu J, Li R. Placental and plasma early predictive biomarkers for gestational diabetes mellitus. *Proteomics Clin Appl*. 2022;16(4):e2200001.

89 Lu S, Lu T, Zhang J, et al. CD248 promotes migration and metastasis of osteosarcoma through ITGB1-mediated FAK-paxillin pathway activation. *BMC Cancer*. 2023;23(1):290.

90 Kang L, Ayala JE, Lee-Young RS, et al. Diet-induced muscle insulin resistance is associated with extracellular matrix remodeling and interaction with integrin alpha2beta1 in mice. *Diabetes*. 2011;60(2):416–426.

91 Luk CT, Shi SY, Cai EP, et al. FAK signalling controls insulin sensitivity through regulation of adipocyte survival. *Nat Commun*. 2017;8:14360.

92 Sulzmaier FJ, Jean C, Schlaepfer DD. FAK in cancer: mechanistic findings and clinical applications. *Nat Rev Cancer*. 2014;14(9):598–610.

93 Pietrzyk L, Wdowiak P. Endosialin (TEM1) as a diagnostic, progression, and prognostic serum marker for patients with colorectal cancer-A preliminary study. *Cancer Control*. 2020;27(1):1073274820903351.

94 Khan KA, McMurray JL, Mohammed F, Bicknell R. C-type lectin domain group 14 proteins in vascular biology, cancer and inflammation. *FEBS J*. 2019;286(17):3299–3332.

95 Teicher BA. CD248: a therapeutic target in cancer and fibrotic diseases. *Oncotarget*. 2019;10(9):993–1009.

96 Brown KA, Scherer PE. Update on adipose tissue and cancer. *Endocr Rev*. 2023;44(6):961–974.

97 Ni L, Yuan C, Wu X. Endoplasmic reticulum stress in diabetic nephrology: regulation, pathological role, and therapeutic potential. *Oxid Med Cell Longev*. 2021;2021:7277966.

98 Fujimoto D, Kuwabara T, Hata Y, et al. Suppressed ER-associated degradation by intraglomerular cross talk between mesangial cells and podocytes causes podocyte injury in diabetic kidney disease. *FASEB J*. 2020;34(11):15577–15590.

99 Krishnan S, Manoharan J, Wang H, et al. CD248 induces a maladaptive unfolded protein response in diabetic kidney disease. *Kidney Int*. 2023;103(2):304–319.

100 Wang H, Karnati S, Madhusudhan T. Regulation of the homeostatic unfolded protein response in diabetic nephropathy. *Pharmaceuticals*. 2022;15(4).

101 Dungan KM, Braithwaite SS, Preiser JC. Stress hyperglycaemia. *Lancet*. 2009;373(9677):1798–1807.

102 Rivas AM, Nugent K. Hyperglycemia, insulin, and insulin resistance in sepsis. *Am J Med Sci*. 2021;361(3):297–302.

103 Wang L, Wang M, Du J, Gong ZC. Intensive insulin therapy in sepsis patients: better data enables better intervention. *Heliyon*. 2023;9(3):e14063.

104 Shi J, Fan J, Su Q, Yang Z. Cytokines and abnormal glucose and lipid metabolism. *Front Endocrinol*. 2019;10:703.

105 Suresh Babu S, Valdez Y, Xu A, et al. TGFbeta-mediated suppression of CD248 in non-cancer cells via canonical Smad-dependent signaling pathways is uncoupled in cancer cells. *BMC Cancer*. 2014;14:113.

106 Rath P, Ranjan A, Chauhan A, et al. A critical review on role of available synthetic drugs and phytochemicals in insulin resistance treatment by targeting PTP1B. *Appl Biochem Biotechnol*. 2022;194(10):4683–4701.

107 Ito Y, Sun R, Yagimuma H, et al. Protein tyrosine phosphatase 1B deficiency improves glucose homeostasis in type 1 diabetes treated with leptin. *Diabetes*. 2022;71(9):1902–1914.

108 Naylor AJ, Azzam E, Smith S, et al. The mesenchymal stem cell marker CD248 (endosialin) is a negative regulator of bone formation in mice. *Arthritis Rheum*. 2012;64(10):3334–3343.

109 Liu S, Han D, Xu C, et al. Antibody-drug conjugates targeting CD248 inhibits liver fibrosis through specific killing on myofibroblasts. *Mol Med*. 2022;28(1):37.

110 Norris RE, Fox E, Reid JM, et al. Phase 1 trial of ontuxizumab (MORAb-004) in children with relapsed or refractory solid tumors: a report from the Children's Oncology Group Phase 1 Pilot Consortium (ADVL1213). *Pediatr Blood Cancer*. 2018;65(5):e26944.

111 Jones RL, Chawla SP, Attia S, et al. A phase 1 and randomized controlled phase 2 trial of the safety and efficacy of the combination of gemcitabine and docetaxel with ontuxizumab (MORAb-004) in metastatic soft-tissue sarcomas. *Cancer*. 2019;125(14):2445–2454.

112 Di Benedetto P, Ruscitti P, Liakouli V, Del Galdo F, Giacomelli R, Cipriani P. Linking myofibroblast generation and microvascular alteration: the role of CD248 from pathogenesis to therapeutic target (Review). *Mol Med Rep*. 2019;20(2):1488–1498.

113 Kondo Y, Honoki K, Kishi S, et al. Endosialin/CD248 may be a potential therapeutic target to prevent the invasion and metastasis in osteosarcoma. *Oncol Lett*. 2022;23(2):42.